A New Paradigm for Concentric Eyewall Formation In Tropical Cyclones

Chun-Chieh Wu

Department of Atmospheric Sciences, National Taiwan University, Taipei, Taiwan

Collaborators: Yi-Hsuan Huang and Guo-Yuan Lien (NTU)
Michael T. Montgomery (NPS)

Typhoon Workshop
Kesen'numa Oshima, Japan
(27 August, 2012)

Acknowledging collaborators in DOTSTAR and T-PARC
Grants: NSC, CWB, RCEC/Academia Sinica, ONR

易致災環境

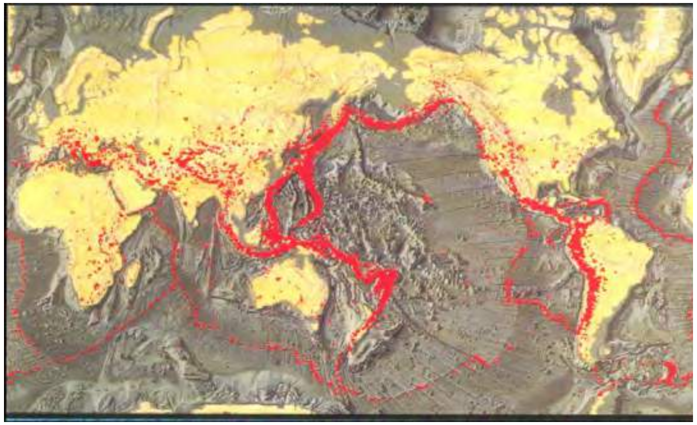

Pacific Ring of Fire

circum-Pacific seismic belt

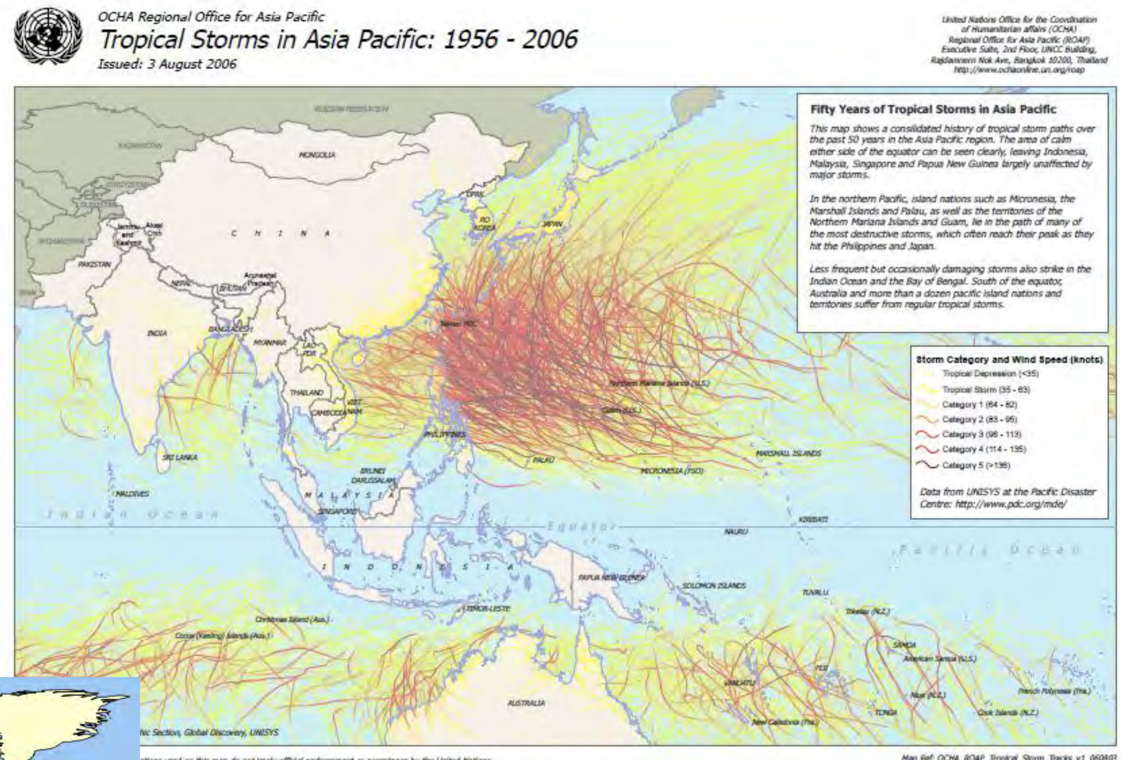

Typhoon Alley

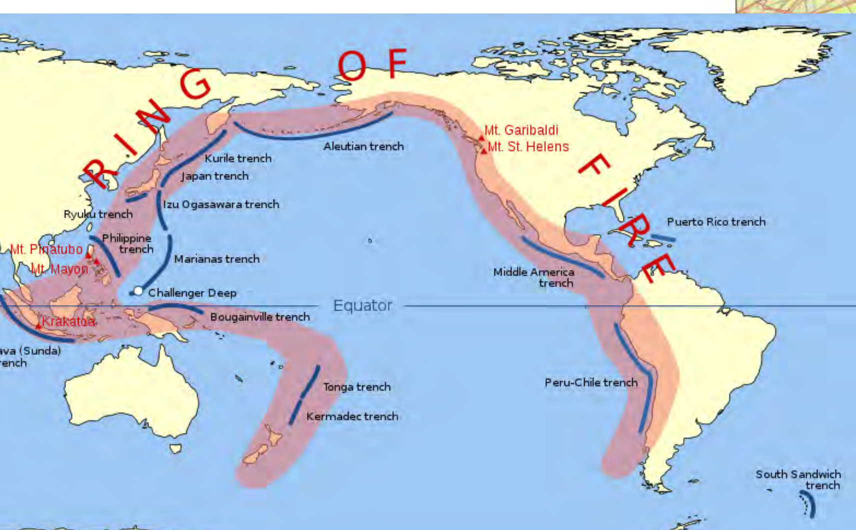

452 volcanoes, 75% of the world’s active and dormant volcanoes

英國風險管理顧問公司Maplecroft於最新公布之“2011年天然災害風險圖輯(the Natural Hazards Risk Atlas 2011 NR)”台灣經濟活動之絕對災害風險指標(Absolute Economic Exposure Index)列為全球第四，與美國、日本與中國並列為具有極端風險之國家。

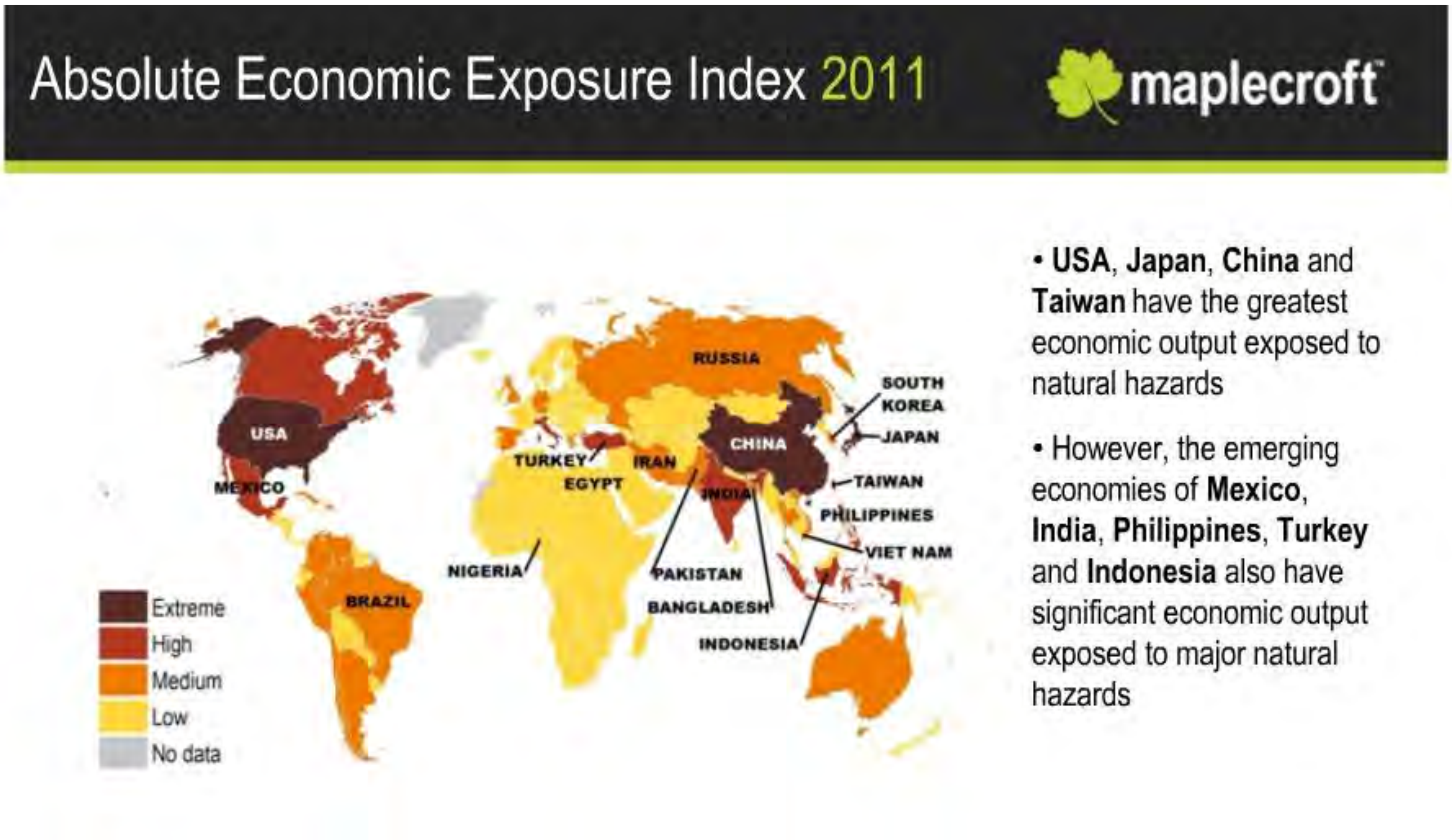

颱風－流體動力學在大自然所展現的絕妙實例

Beauty and the Beast

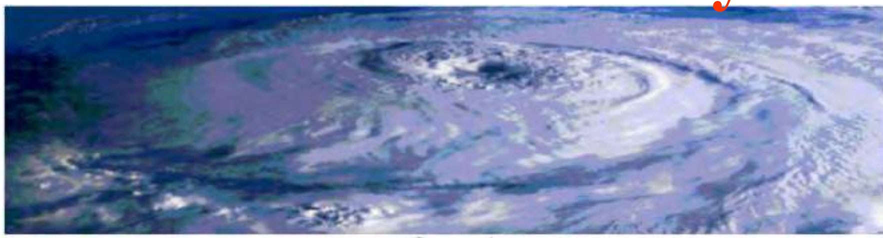

從太空看颱風

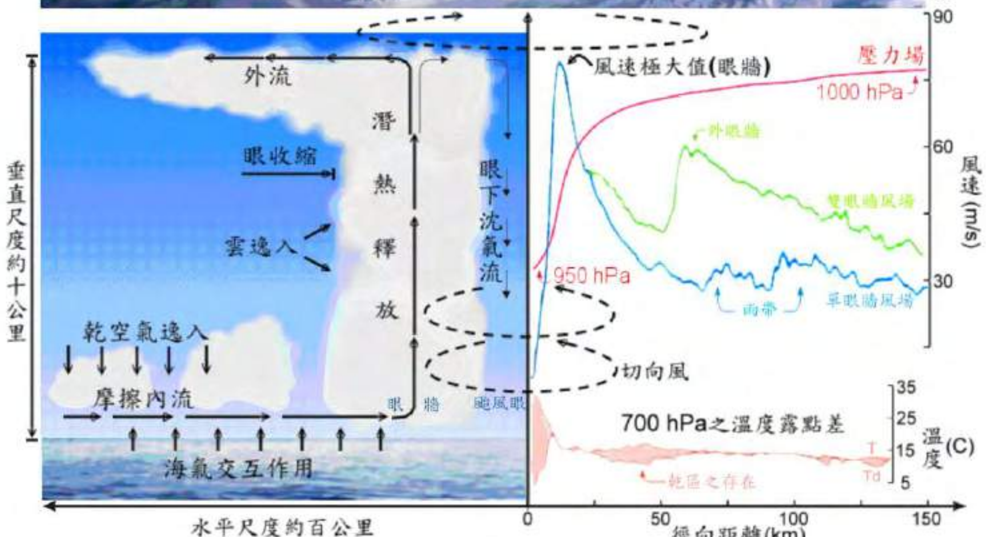

- 高速旋轉流 (highly swirling)
- 強烈輻合輻散流 (strong convergence)
- 劇烈濕對流 (deep moist convection)
- 快速大氣—海洋交互作用 (fast air-sea interaction)
- 多重尺度交互作用 (multi-scale interaction)
- 地形效應 (terrain effect)

(Chun-Chieh Wu: 2002-2009)

(Wu et al. 2002, WF)

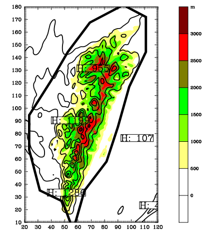

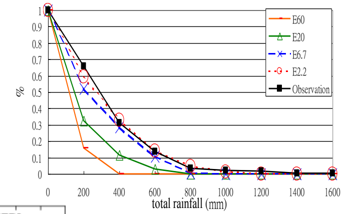

(Wu et al. 2009a, b, MWR)

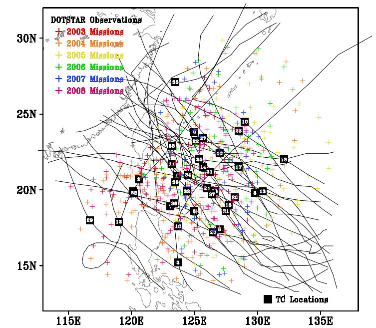

(Wu et al. 2007a JAS)

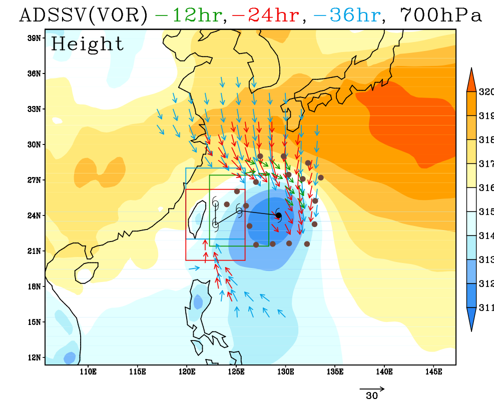

(Wu et al. 2006, JAS)

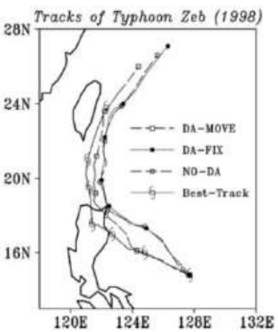

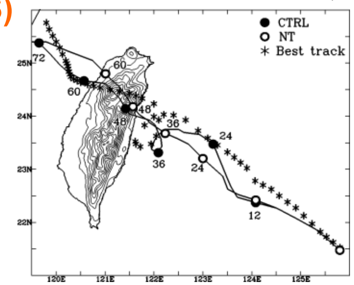

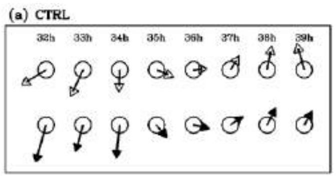

(Jian and Wu 2008, MWR)

- Targeted observation in DOTSTAR
- Typhoon intensity eyewall dynamics
- Typhoon-terrain interaction
- Typhoon movement
- Typhoon rainfall
- Typhoon-ocean interaction
- Typhoon-climate

(Wu et al. 2009c, MWR)

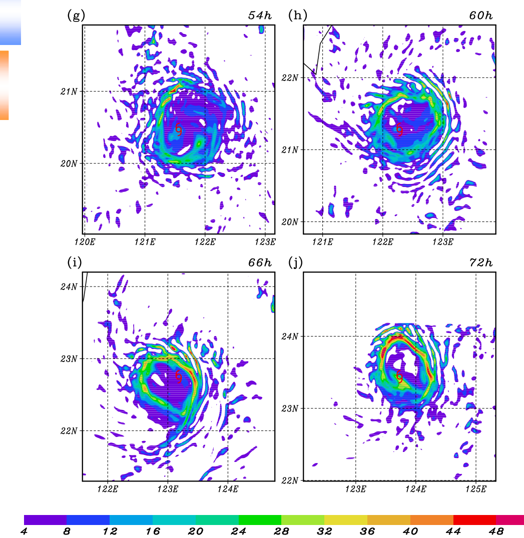

(Wu et al. 2003, MWR)

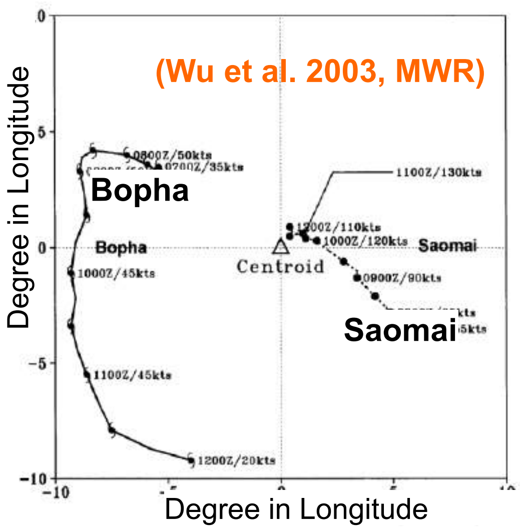

(Wu et al. 2007b, JAS)

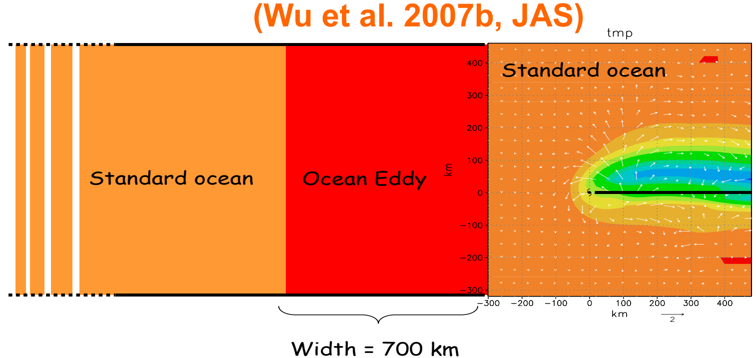

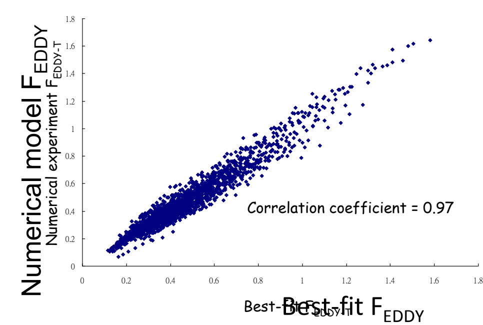

Long-term decreasing trend in TC track prediction errors

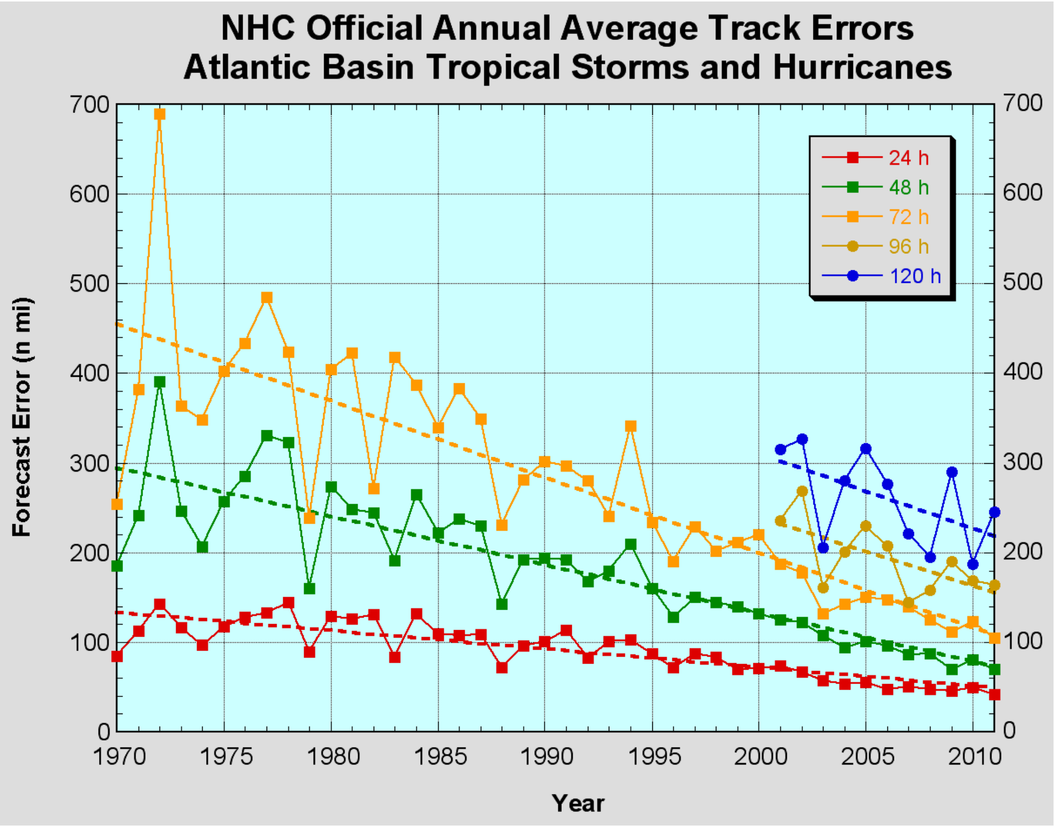

From NHC

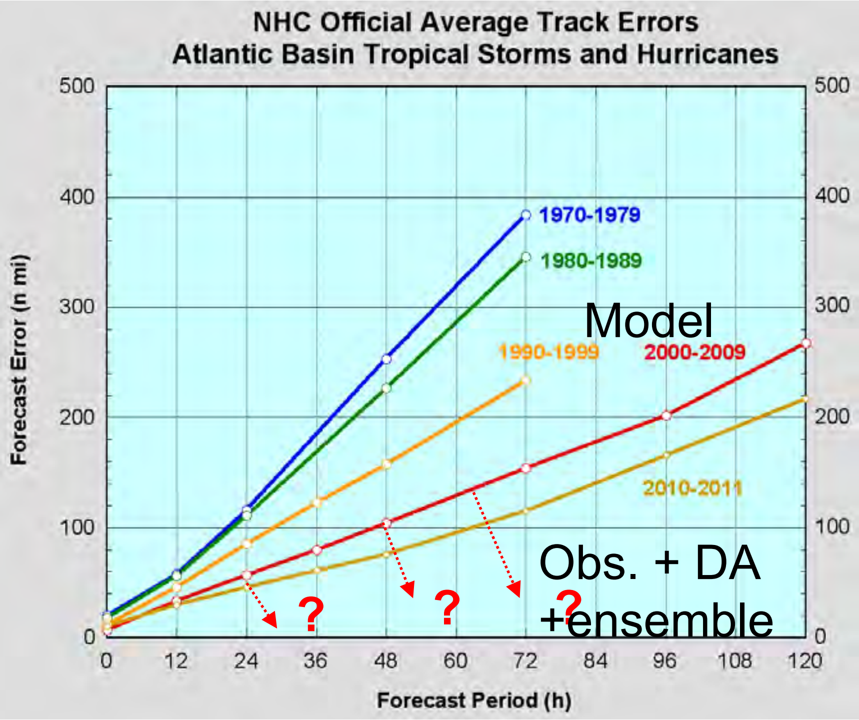

Push the limit of predictability?

Very limited progress in TC intensity prediction

From NHC

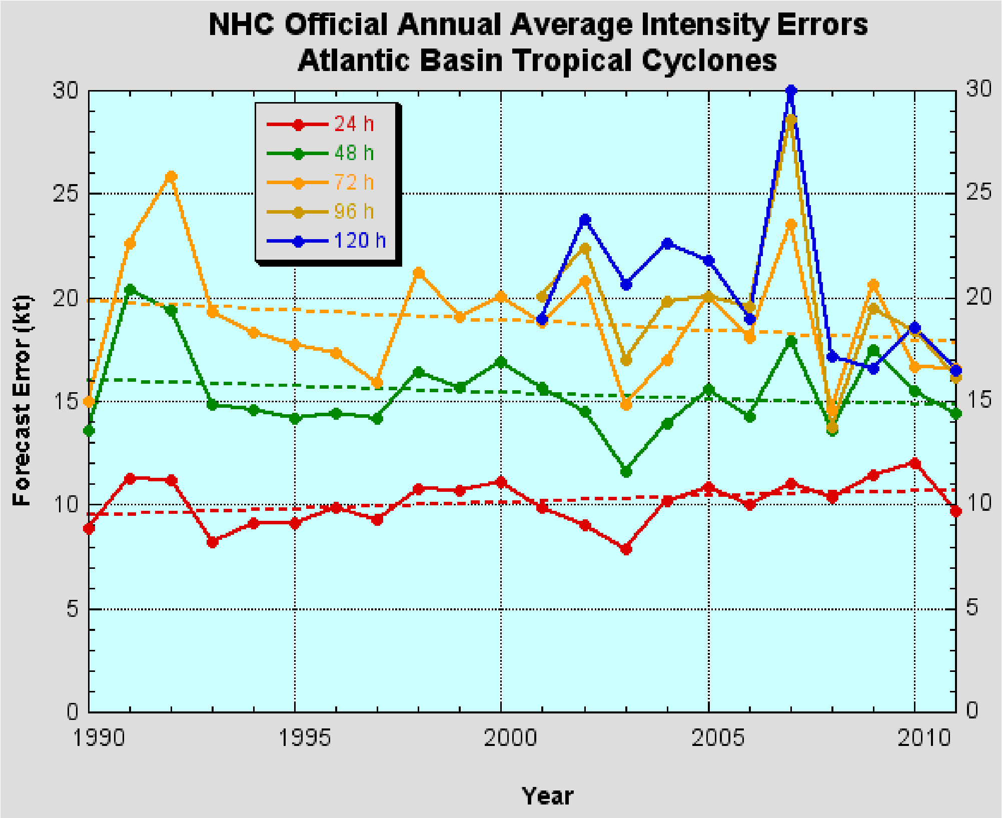

Internal dynamics – VRW, spiral rainbands, mesoscale vortices, eyewall processes

Environmental control – shear, trough-interaction (Wang and Wu 2004)

Boundary processes – sfc. fluxes, ocean mixing, sea spray, waves, land/topography

Improving the understanding and prediction of the TC systems

(in memory of Dr. Yoshio Kurihara)

Key issues:

- dynamics
- observation
- model simulation/data assimilation

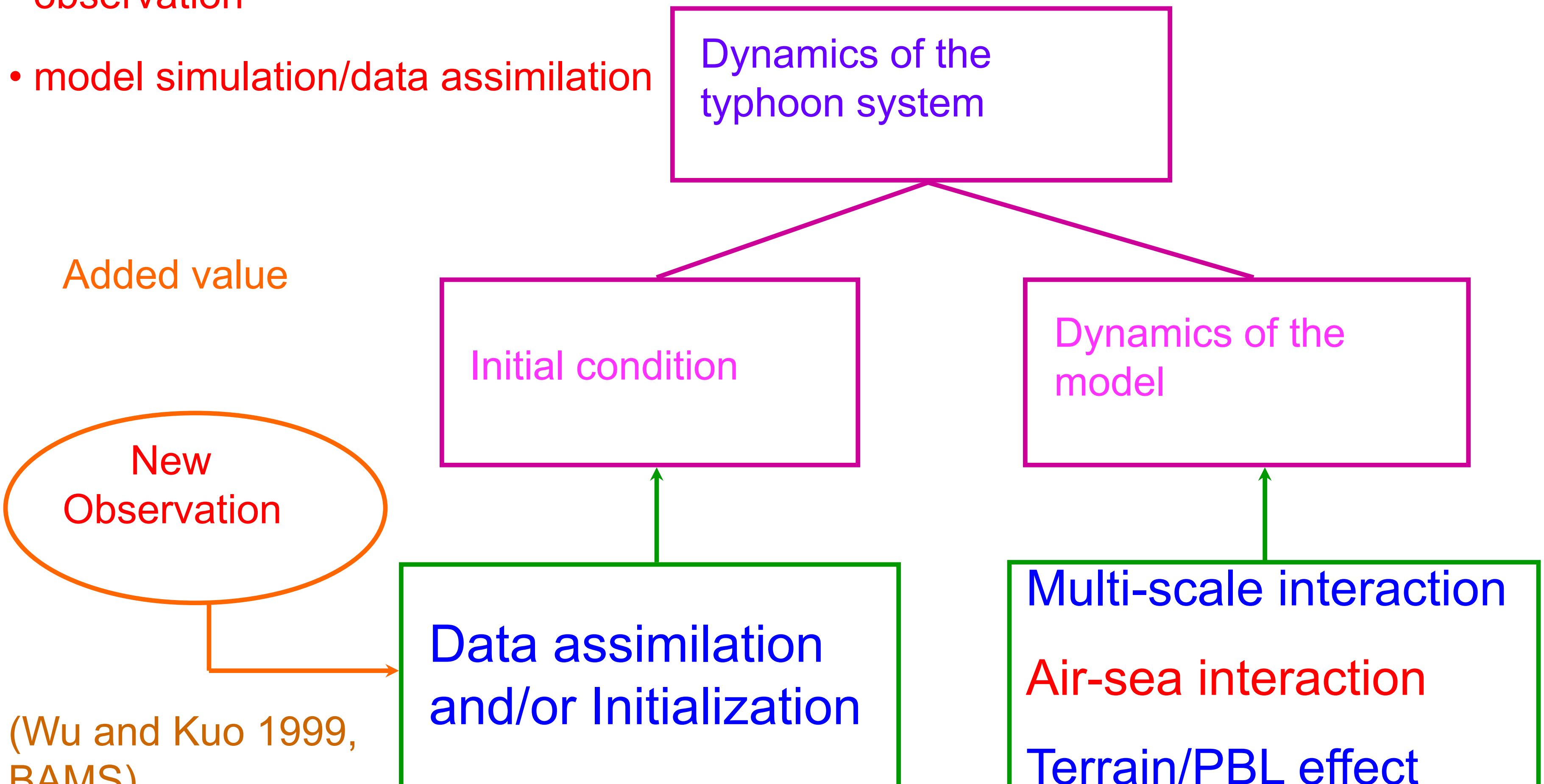

Outline

- Observation:
  DOTSTAR, T-PARC and Typhoon Sinlaku (2008)
  (Wu et al. 2012a, MWR)
- Data Assimilation and simulations:
  EnKF data assimilation and analyses
  (Wu et al. 2010, JAS; Wu et al. 2012b, MWR)
- Dynamical Analysis:
  Axisymmetric dynamical processes
  (Huang et al. 2012, JAS)

Objectives

Part I

- Constructing a dataset for Typhoon Sinlaku by using T-PARC data and a new vortex initialization method via the WRF model.
- **Showing the evolution of the concentric eyewall cycle in terms of different parameters.**
- Studying the impact of the amount of the assimilated data.

Part II

- **Investigating potential precursors to SEF and providing a corresponding dynamical interpretation.**
- **Proposing a new pathway to SEF based on an axisymmetric view.** ***(Unbalanced response within and just above the boundary layer.)***

Part III

- **Validating the presenting pathway in the data-denial experiments.**

➔ ***Investigation of the dynamics of concentric eyewall formation***

Dropwindsonde Observations for Typhoon Surveillance near the Taiwan Region (DOTSTAR, 2003 – present)

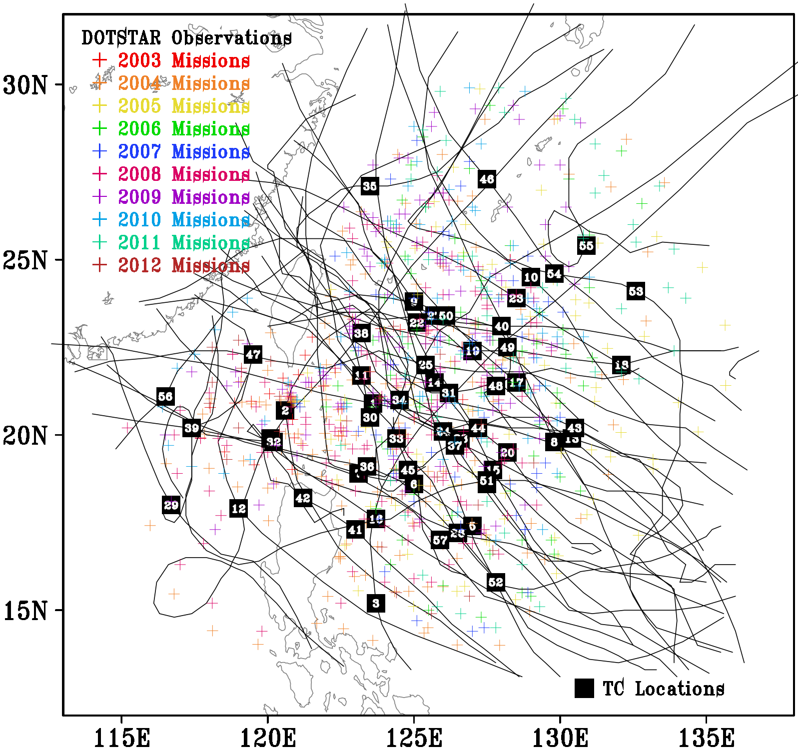

Up to present, 61 missions have been conducted in DOTSTAR for 47 typhoons, with 993 dropwindsondes deployed during the 329 flight hours.

42 typhoons affecting Taiwan

32 typhoons affecting (mainland) China

9 typhoons affecting Japan

5 typhoons affecting Korea

14 typhoons affecting Philippines

- Useful real-time data available to major operational forecast centers

- Positive impact to the track forecasts to models in major operation centers (NCEP/GFS, FNMOC/NOGAPS, JMA/GSM)

Wu et al. (2005 BAMS, 2007a JAS, 2007b WF, 2009a,b,c MWR), Chou and Wu (2008 MWR), Chen et al. (2009 MWR, JAS), Yamaguchi et al. (2009 MWR), Chou et al. (2010 JGR)

- Targeted observation

Weissmann et al. (2010 MWR)

THORPEX-PARC Experiments (2008) and Collaborating Efforts

Understand the lifecycle of TC and improve its predictability –

- Genesis
- Intensity and structure change
- Recurvature (targeted obs.)
- Extra-tropical transition (ET)

Elsberry and Harr (2009)

Motivations

- Typhoon Sinlaku (2008) is a case in point under T-PARC (THORPEX – Pacific Asian Regional Campaign) with ***the most abundant flight observations***.
- ***The new method for TC initialization*** based on EnKF data assimilation and the WRF model

  (Details in **Wu et al. 2010, JAS**)

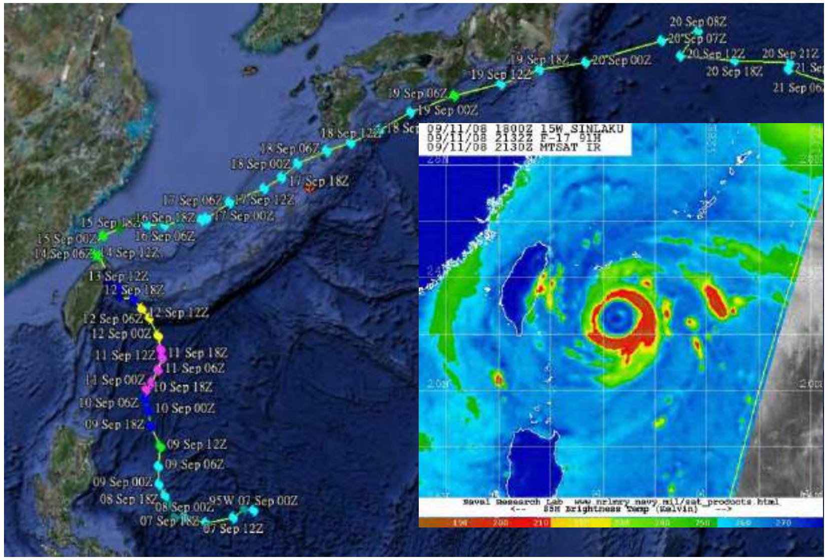

Objectives

- To construct ***a high-spatio-temporal model dataset*** for Sinlaku from Sept. 9 to 13. (**Wu et al. 2012b, Part I, MWR**)
- To investigate the dynamics of the ***concentric eyewall formation and cycle*** in Sinlaku. (**Huang et al., 2012, Part II, JAS**)

Data

THORPEX Pacific Asian Regional Campaign
(*T-PARC*)

- 2008/09/08 17:00 ~ 09/13 03:00 UTC

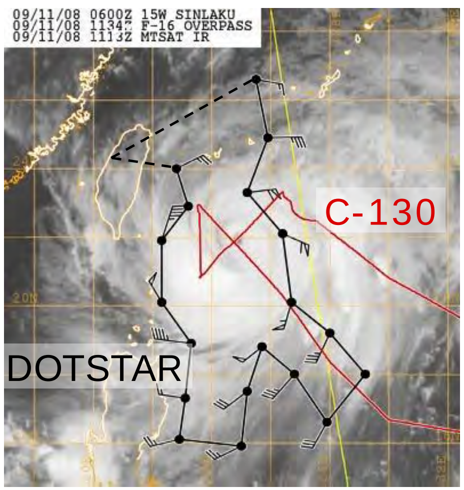

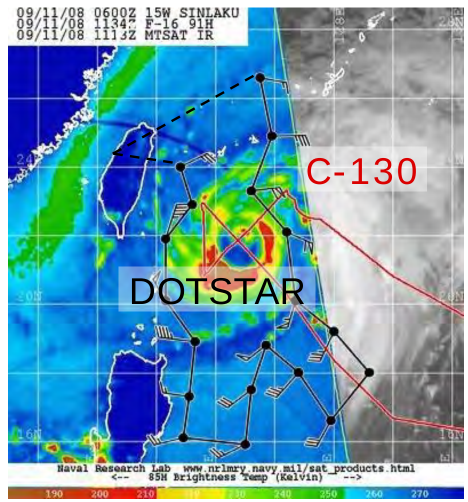

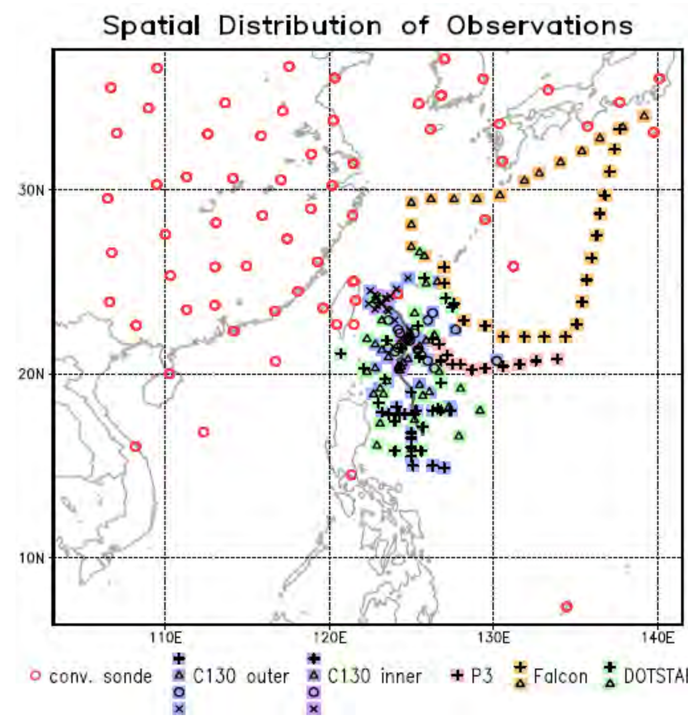

9 flight missions with 159 dropwindsondes

<table>
<tr><th rowspan="3"></th><th rowspan="3">Conv. radiosonde</th><th colspan="5">Dropwindsondes</th></tr>
<tr><th rowspan="2">DOTSTAR ASTRA</th><th rowspan="2">DLR Falcon</th><th rowspan="2">NRL P-3</th><th colspan="2">USAF C-130</th></tr>
<tr><th>Inner core</th><th>Others</th></tr>
<tr><td rowspan="2">Total available</td><td rowspan="2">623</td><td rowspan="2">36
(2 flights)</td><td rowspan="2">34
(2 flight)</td><td rowspan="2">12
(1 flight)</td><td>20</td><td>57</td></tr>
<tr><td colspan="2">(4 flights)</td></tr>
</table>

(Wu et al. 2012b, MWR)

Methodology

EnKF data assimilation/ WRF model

- Observation operators related to TCs (Wu et al. 2010a)
  center position / motion vector/
  axisymmetric wind structure
  – 3 hour best track data
  – TC radius (34, 50 kts) data from JTWC.
  – Surface wind from the T-PARC data (dropsondes and SFMR)

- Rapid update Cycle (RUC): 30 mins
- horizontal resolution : 5 km
- 35 vertical layers
- 30-min output interval
- 28 ensemble members

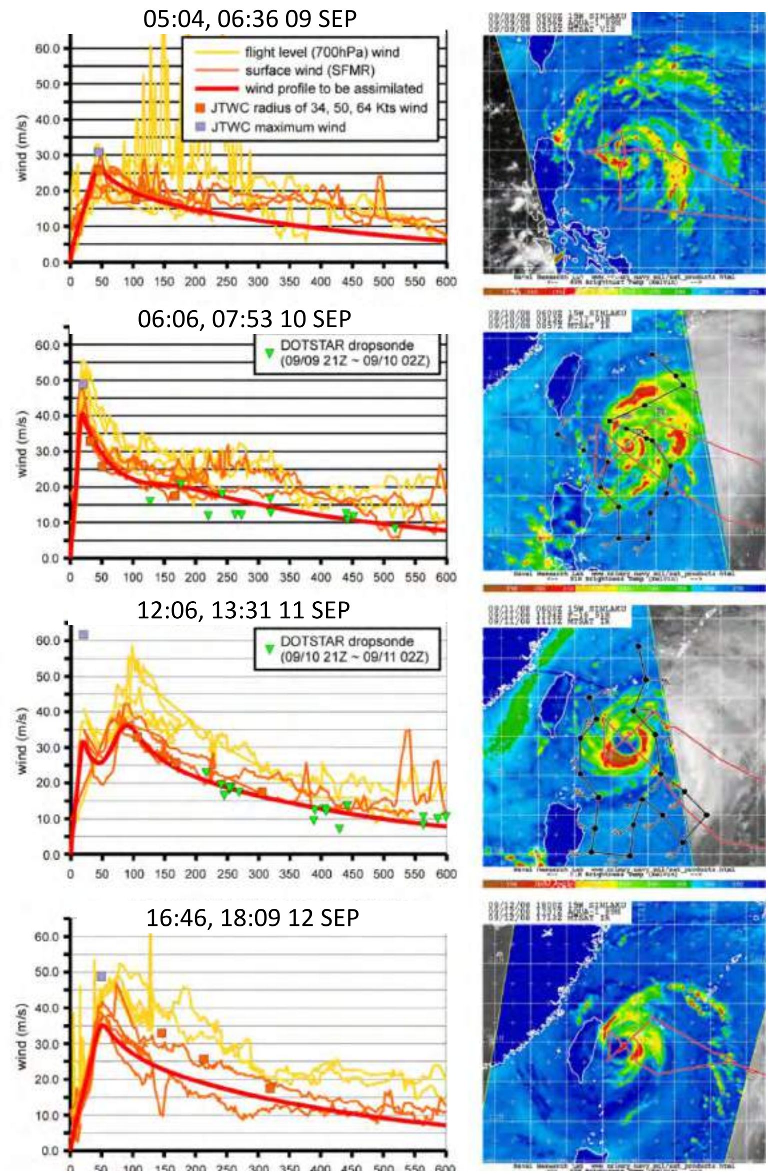

(Wu et al. 2012b, MWR)

Assimilation of Tropical Cyclone Track and Structure Based on the Ensemble Kalman Filter (EnKF)

- Observation data for Typhoon Fung-wong
  - Three-hour track data from CWB, interpolated to 30 minutes interval by cubic-spline method
  - TC radius (34, 50 kts) data from JTWC.
  - **DOTSTAR** (Wu et al. 2005, 2007) **surface wind data** (MBL150, Franklin 2003) on 26 July. 1200 UTC (final time of the initialization period).

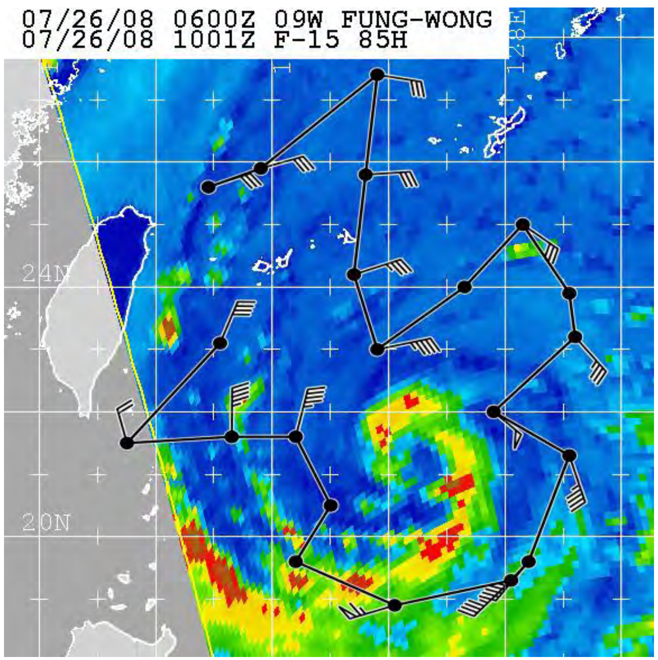

(Wu et al. 2010, JAS)

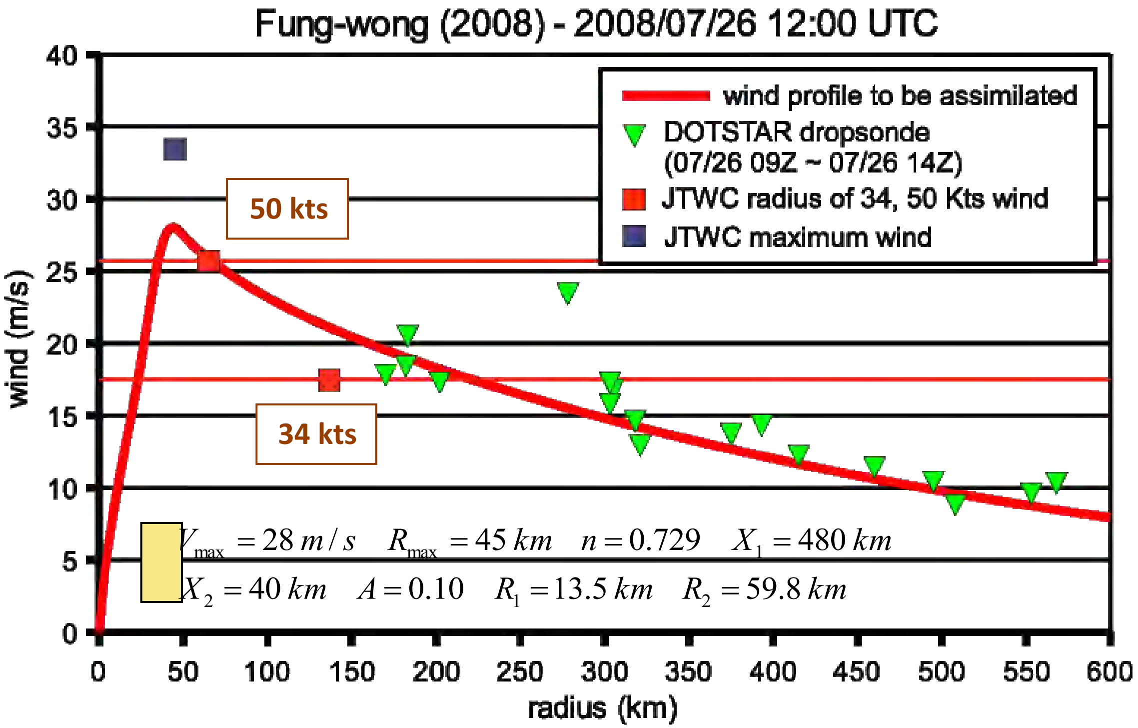

After Willoughby et al. (2006)

• Results – Wind and SLP fields

CTRL experiment

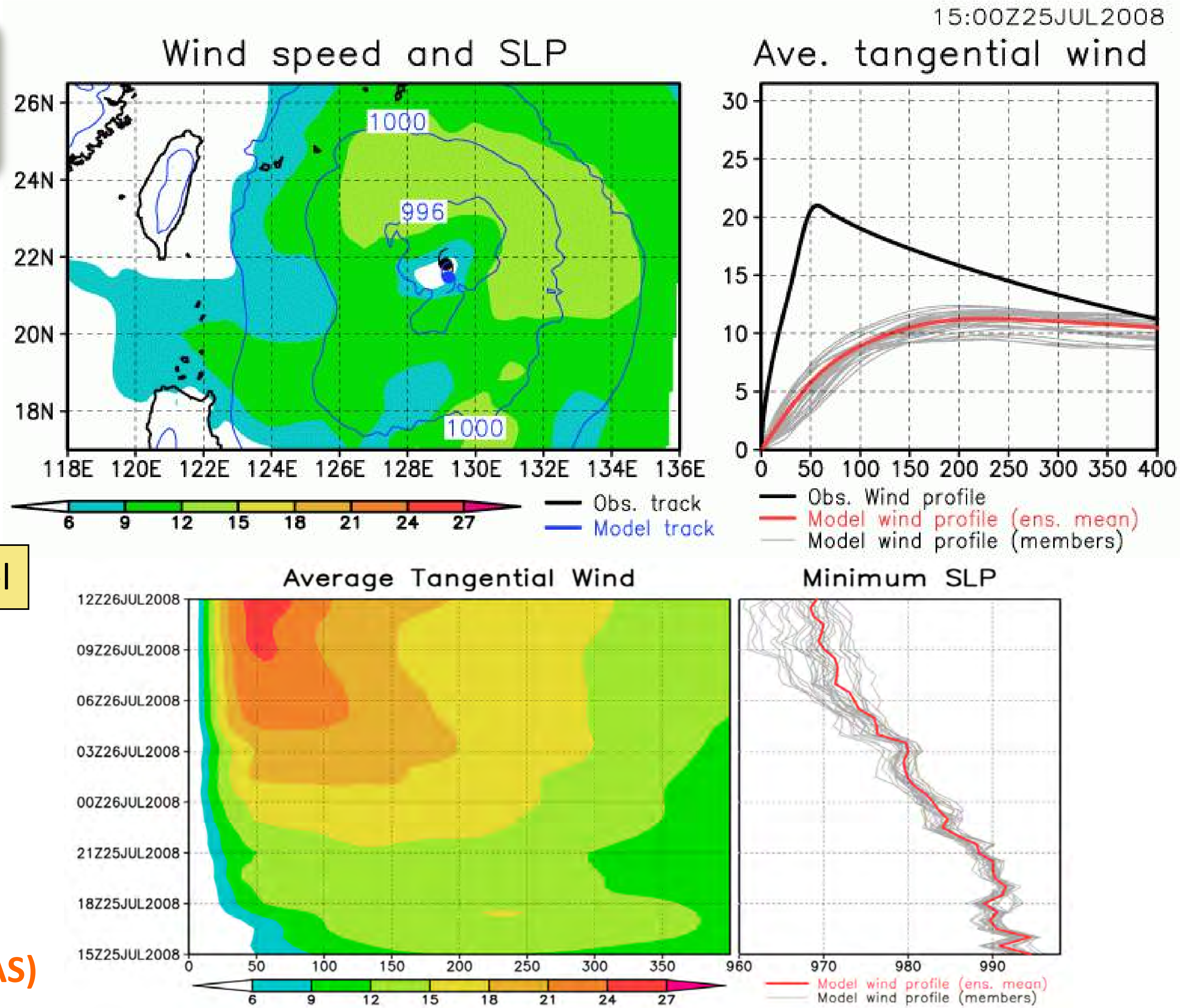

Lowest sigma level

(Wu et al. 2010, JAS)

Vertical structure after the initialization

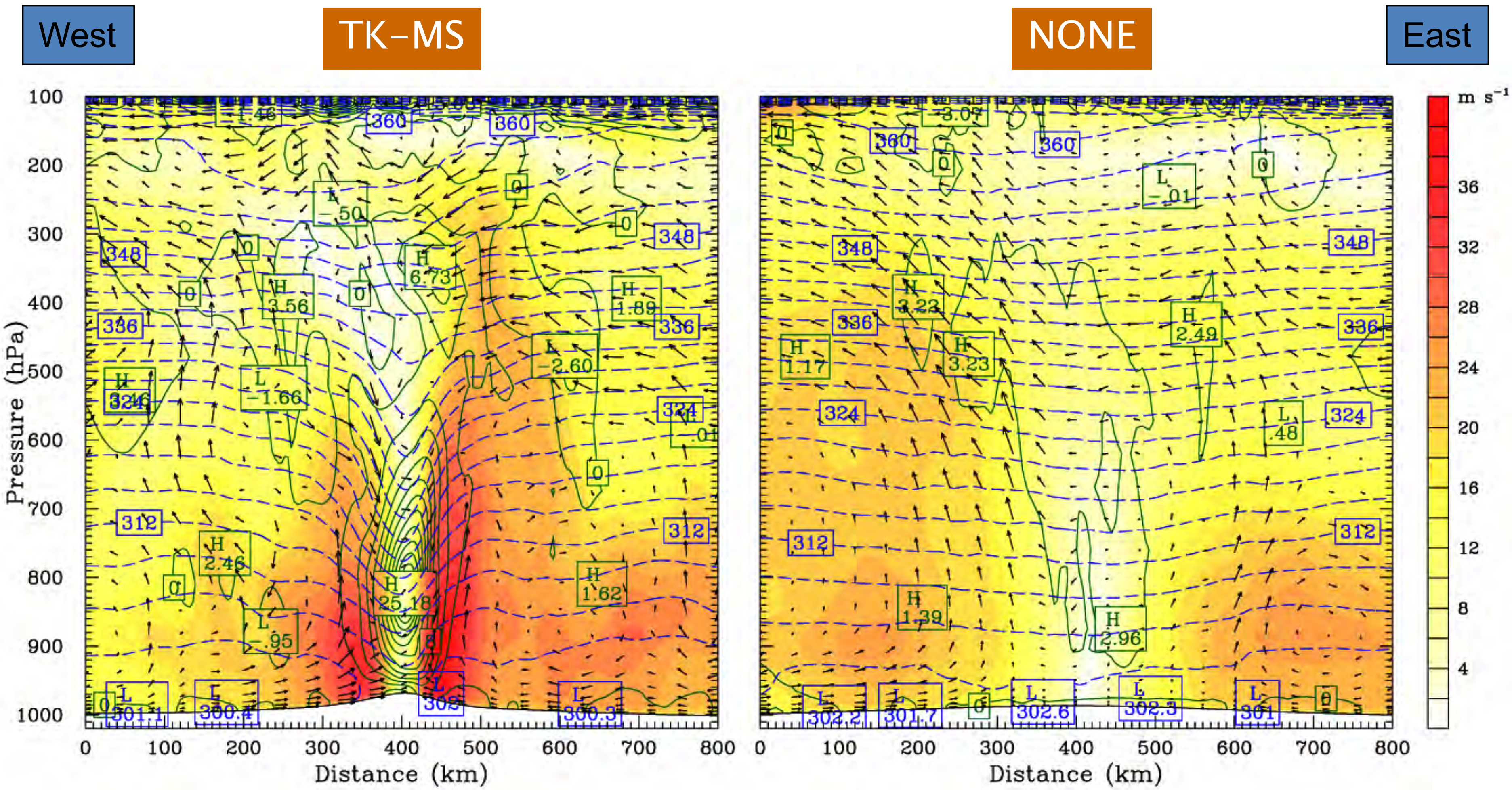

(Wu et al. 2010, JAS)

Time-radius plots of the azimuthally-mean structure

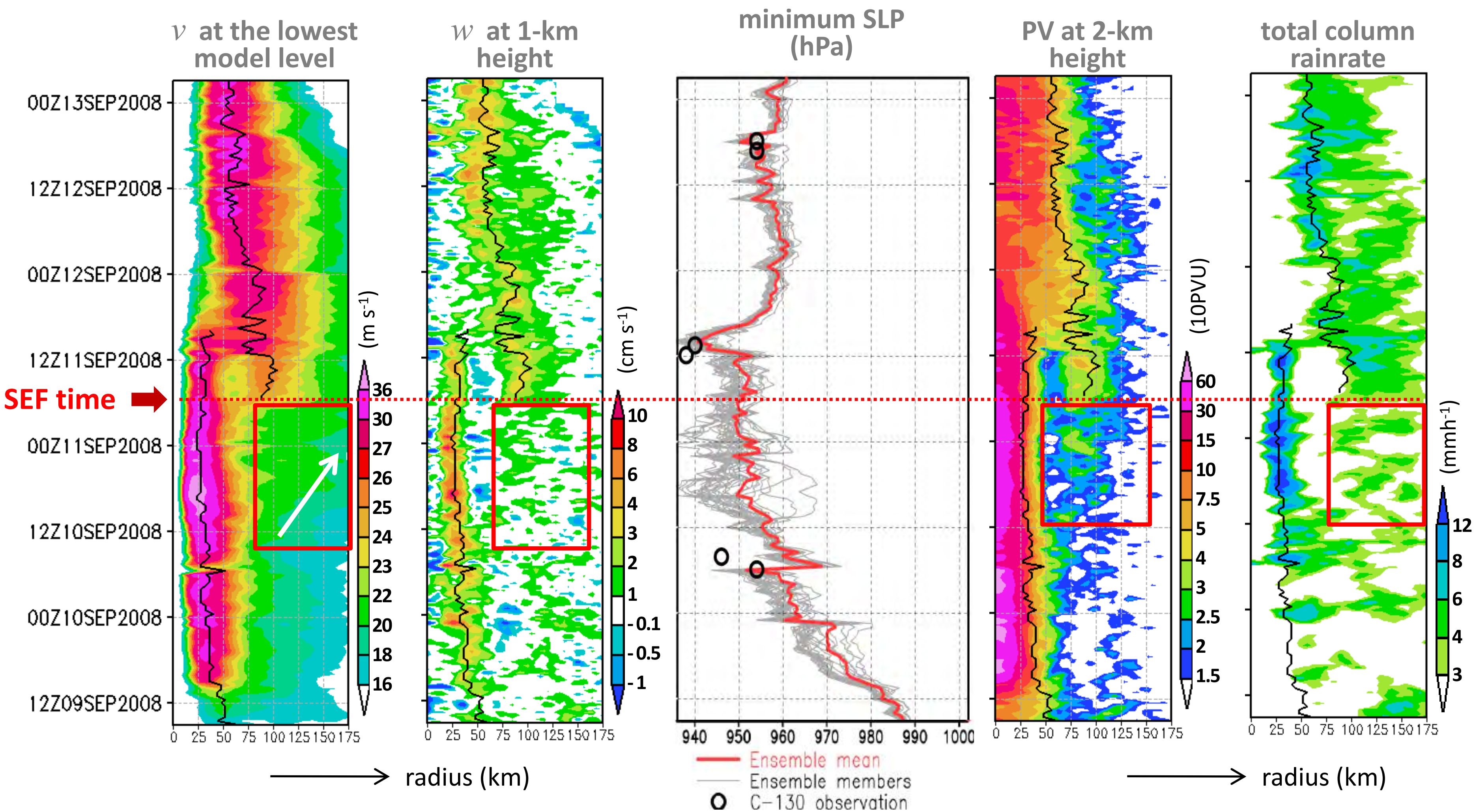

SEF time: a persistent secondary maximum in *V* at the lowest model level

Hr -1 : 1 h prior to SEF ; Hr 0 : SEF time ; Hr 1: 1 h after SEF

(Wu et al. 2012b, MWR)

Plan view : potential vorticity (PV) at 1-km height

From 0300 UTC 10 SEP (H -28)
To 0900 UTC 12 SEP (H 26)

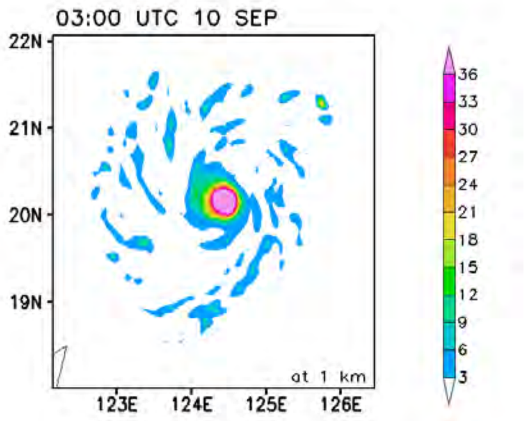

sporadic PV bands/patches

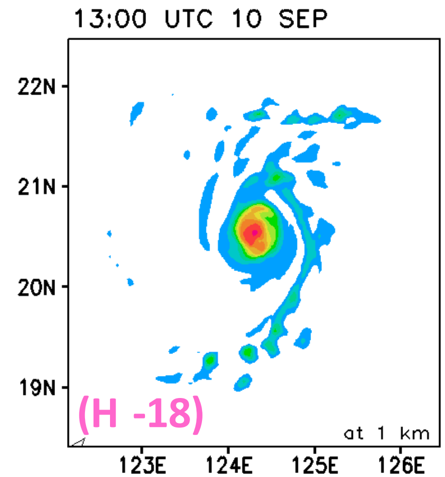

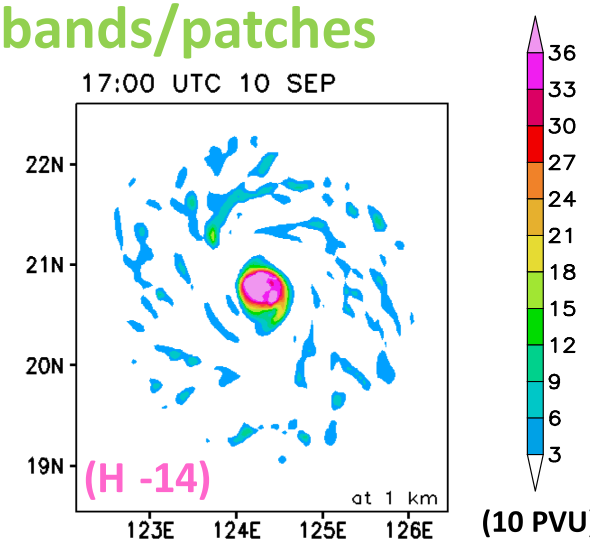

PV bands organize into a PV ring

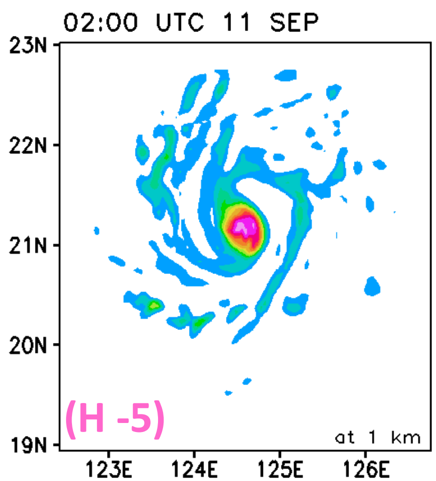

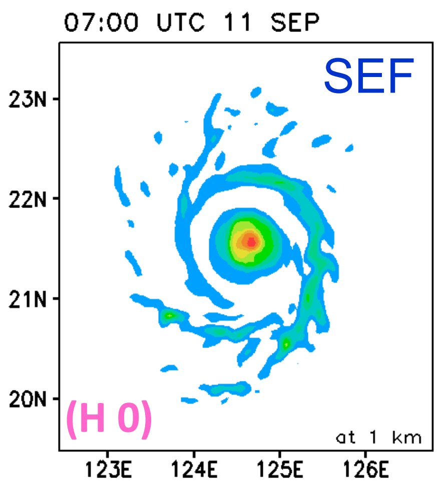

Eyewall replacement

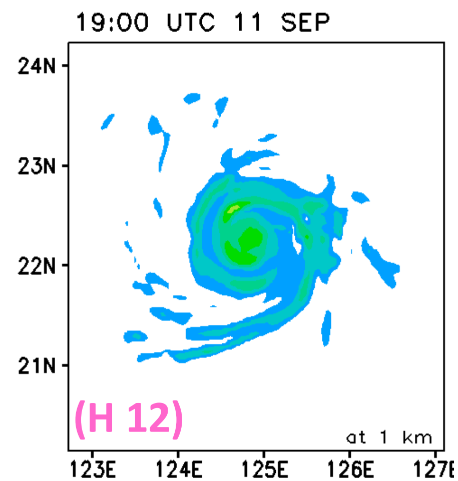

new eyewall

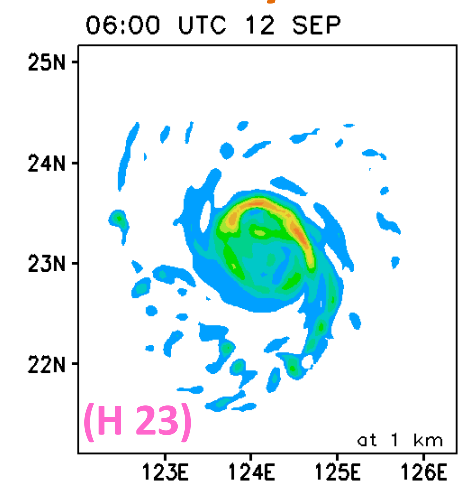

(Plots for ***m11* of CTL**. Those for the ensemble mean of CTL were presented in part I work.) *(Wu et al. 2012b)*

CTL - Radii of local Vmax

All the ensemble members have a similar pathway to SEF and similar ERCs.

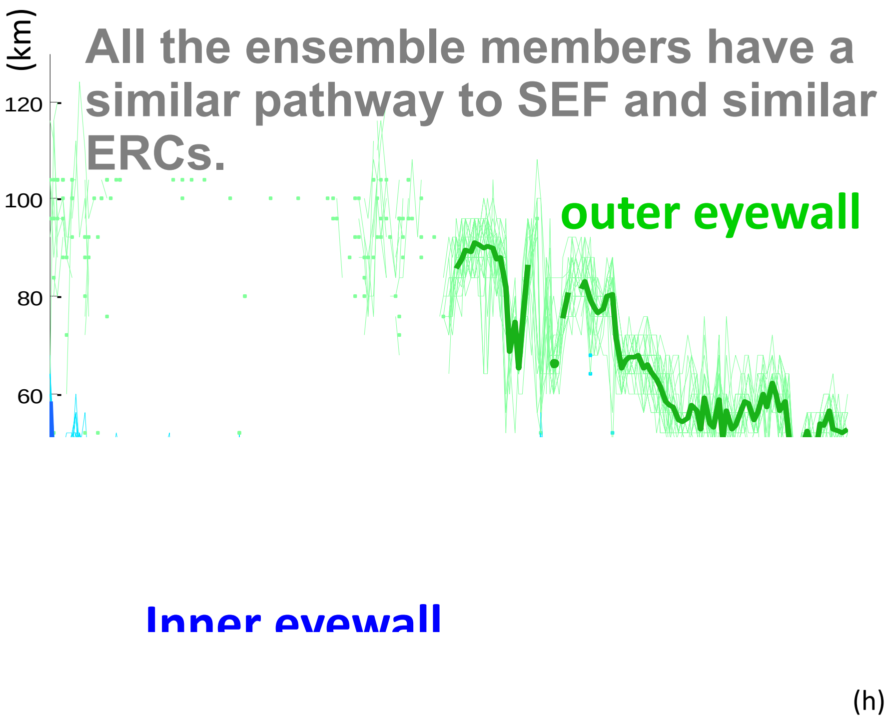

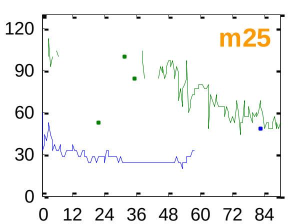

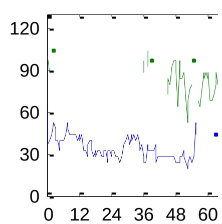

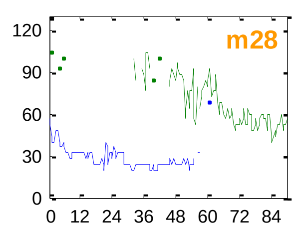

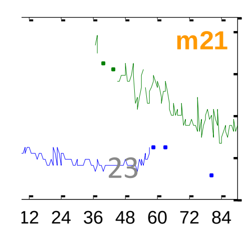

WRF/EnKF, 5-km resolution

(Wu et al. 2012b, MWR)

***Part II** - dynamical analysis (axisymmetric process)*

- **Background review**
- **Motivations**
- **Objectives**
- **A new paradigm for the secondary eyewall formation in terms of the axisymmetric aspect**
  - **Precursors prior to SEF**
  - **Boundary layer inflow evolution**
  - **Dynamical interpretation**
- **Concluding remarks**
- **Ongoing works**
- **Issues to be further addressed**

Review of studies on the secondary eyewall formation

Possible favorable conditions or mechanisms	**References**
Asymmetric due to the storm's motion	Willoughby 1979
Updrafts induced by the downdrafts in the moat	Willoughby 1982
Topographic influence	Hawkins 1983
External eddy angular momentum fluxes and WISHE process	Nong and Emanuel 2003
Ice microphysics (may not be essential for SEF, but has impacts on the SEF time, location and period of ERCs.)	Willoughby et al. 1984; Terwey and Montgomery 2008; Zhou and Wang 2011
High environmental relative humidity	Ortt and Chen 2008; Wang 2009; Hill and Lackmann 2009
Vortex Rossby Waves (VRWs ; e.g., Montgomery and Kallenbach 1997; Brunet and Montgomery 2002; Montgomery and Brunet 2002)	Montgomery and Enagonio 1998; Chen and Yau 2001; Chen et al. 2003; Wang 2002a, b; Corbosiero et al. 2006; Qiu et al. 2010; Abarca and Corbosiero 2011; Martinez et al. 2011
Axisymmetrization process (Melander et al. 1987; McWilliams 1990; Dritschel and Waugh 1992; Fuentes 2004)	Kuo et al. 2004, 2008; Moon et al. 2010 (Moon showed conflicting results)
β-skirt axisymmetrization formation hypothesis	Terwey and Montgomery 2008; Qiu et al. 2010
Unbalanced dynamics: flow response near the top of BL associated with the broadening of the swirling circulation	Wu et al. 2012; Huang et al. 2012
Balanced dynamics: roles of heating and inertial stability	Rozoff et al. 2012

Notable new and different results

Potential intrinsic mechanisms for SEF

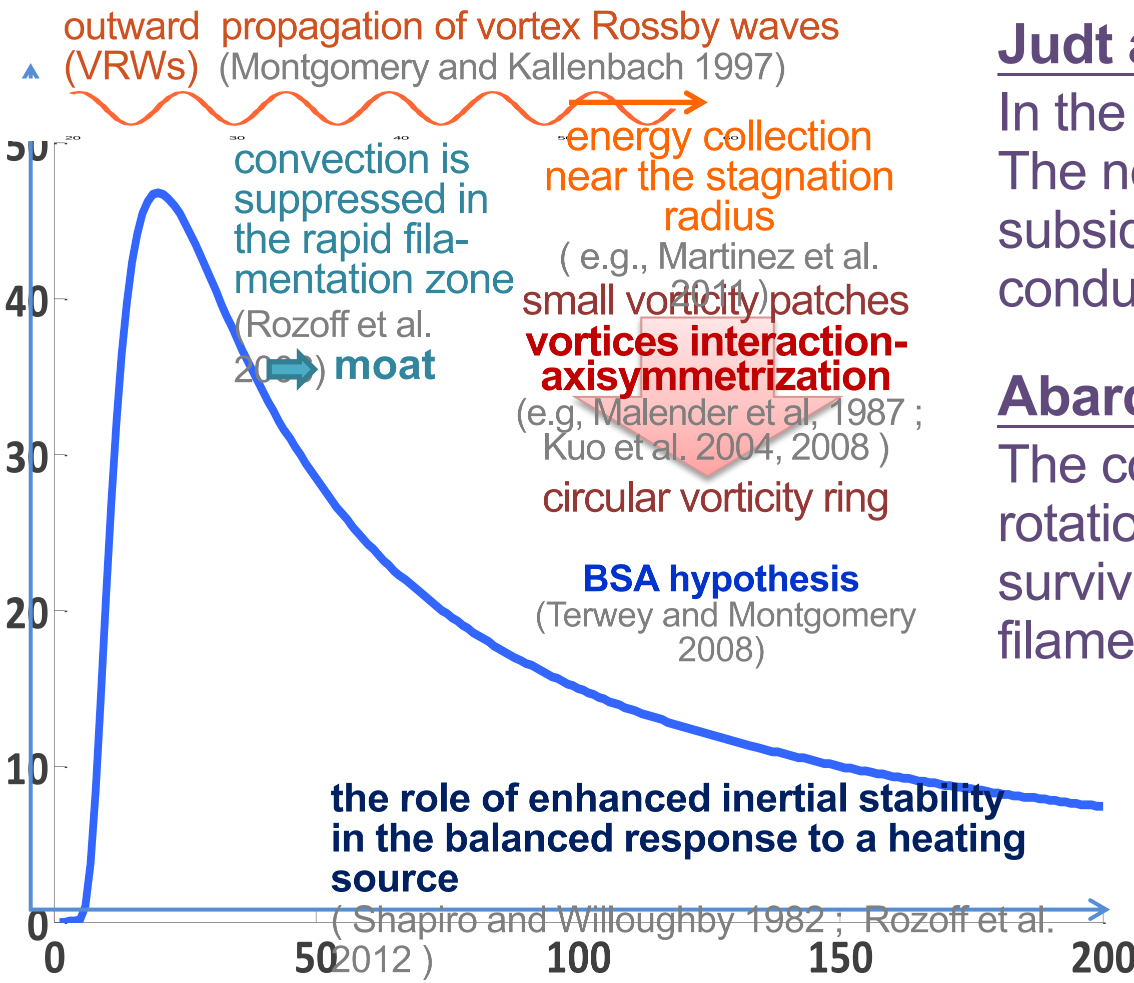

Judt and Chen (2010)

In the moat region:
The near-zero PV gradient, subsidence and straining effect are not conducive for VRWs' activities.

Abarca and Coborsiero (2011)

The convective-coupled VRWs are rotation dominated and thus can survive when passing over a rapid filamentation zone.

Wang (2008)

Inner spiral rainbands occur in the RFZ due to the stabilization and axisymmetrization of high-wavenumber asymmetries by straining deformation.

Moon et al. (2010)

Convection-induced small vorticity dipoles of considerable strength in the 2-D barotropic flow does not lead to a coherent vorticity ring.

Background review (i)

- Secondary eyewall structure is observed relatively common for intense Western Pacific typhoons (surface maximum winds > 120 kts, or Category 4 - 5).

  (Observational studies, e.g., Hawkins and Helveston 2008; and follow-up works)

- It is logical to regard the secondary eyewall formation (SEF) as an intrinsic part of an intense typhoon's lifecycle provided that the environment is not or not sufficiently unfavorable for the storm's development.

Background review (ii)

- From the standpoint of the mean-field dynamics (the azimuthally average around the vortex's circulation center), the deep convection in the eyewall is involved in ***two mechanisms for spinning up the mean vortex*** (Smith et al. 2009).

$$M = rv + \frac{1}{2} f r^2$$

M: absolute angular momentum

$$v = \frac{M}{r} - \frac{1}{2} fr$$

1) Above BL : M is materially conserved

The increase of tangential circulation can be achieved by weak inflow

2) Within the BL: M is not materially conserved

Despite the loss of M in the boundary layer,
if the radial inflow is sufficiently large,
the increase of swirling wind can be achieved .

→ **Emphasis on the convergence of M in the BL**

Schematic diagram on the development of agradient wind

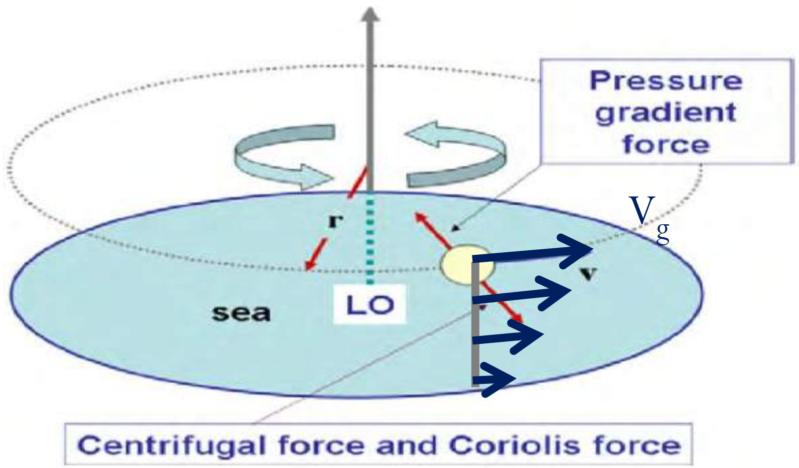

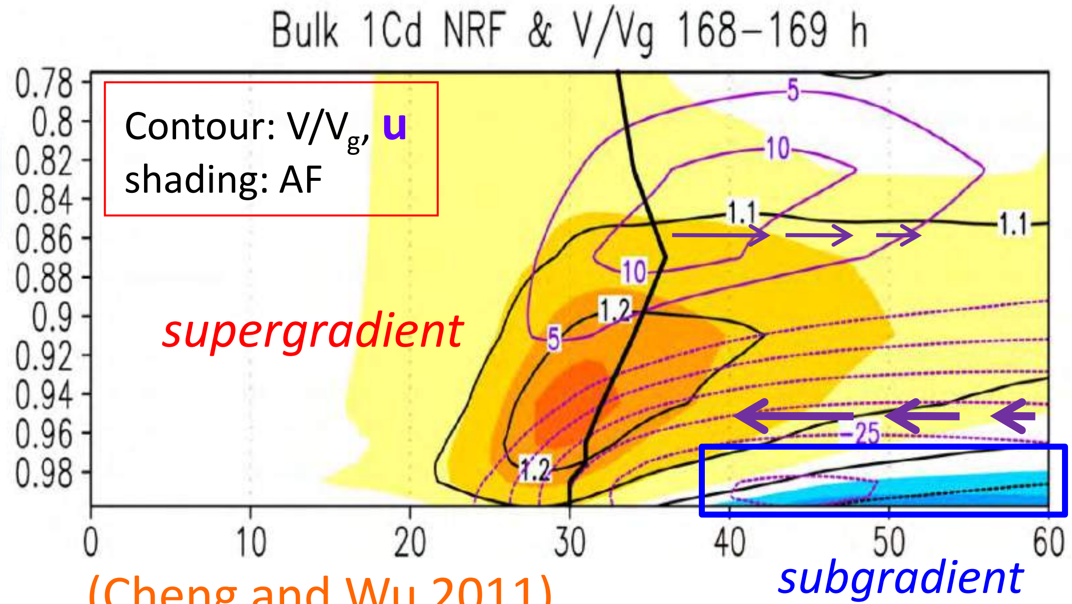

(Cheng and Wu 2011)

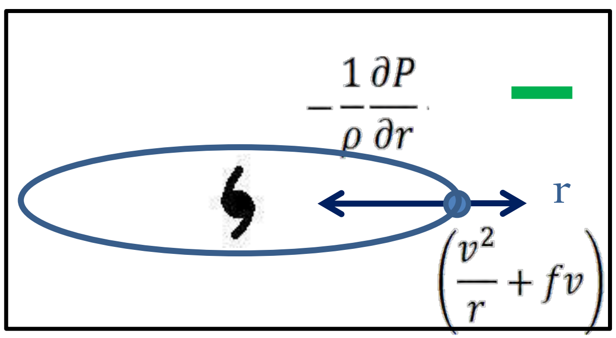

$$\frac{du}{dt} = -\frac{1}{\rho}\frac{\partial P}{\partial r} + \left(\frac{v^2}{r} + fv\right) - Fr$$

Agradient Force (AF)

$$\frac{\partial v}{\partial t} = -u(\zeta + f) - w\frac{\partial v}{\partial z} - Fr$$

$$\zeta = \frac{1}{r}\frac{\partial rv}{\partial r}$$

If V is subgradient (V < Vg), inflow accelerated

Schematic diagram on the development of agradient wind

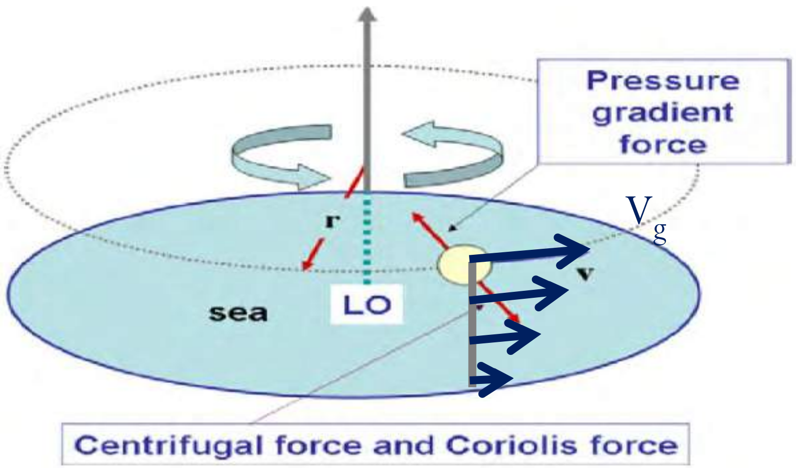

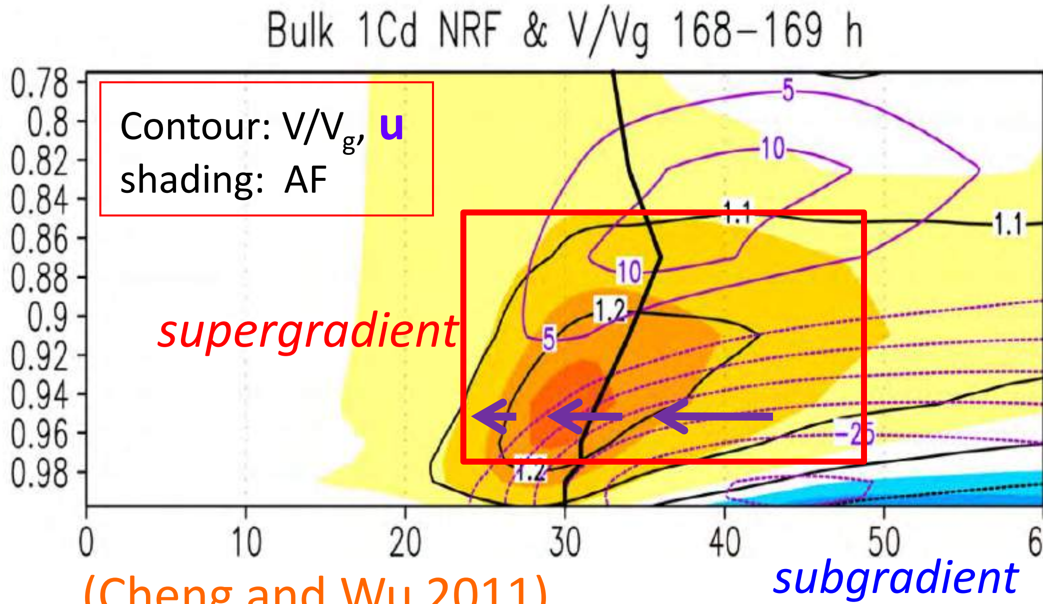

(Cheng and Wu 2011)

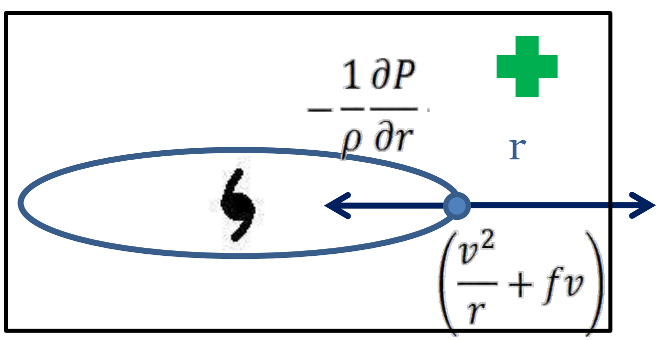

$$\frac{du}{dt} = \underbrace{-\frac{1}{\rho}\frac{\partial P}{\partial r} + \left(\frac{v^2}{r} + fv\right)} - Fr$$

Agradient Force (AF)

$$\frac{\partial v}{\partial t} = -u(\zeta + f) - w\frac{\partial v}{\partial z} - Fr$$

$$\zeta = \frac{1}{r}\frac{\partial rv}{\partial r}$$

If V is supergradient (V > Vg),
inflow decelerated

Background review (iii)

Features found during the tropical cyclone intensification corresponding to this spin-up paradigm (*Smith et al. 2009*)

- A broadening of the outer tangential wind field above and within the boundary layer.

- An amplification of radial inflow in the boundary layer in response to an increased radial pressure gradient near its top associated with the broadening tangential wind field in the outer region of the vortex.

- The generation of persistent supergradient tangential winds in the inner-core boundary layer where the radial wind becomes sufficiently strong.

Motivations (i)

- Given the widely documented association between SEF and increases in storm size, one may anticipate that these two spin-up mechanisms might be important also during SEF.
- Precursory broadening of the outer swirling circulation suggests that an application of the spin-up paradigm to the problem of SEF may serve as a foundation stone for a new SEF pathway.

Motivations (ii)

- Examination prior to SEF and investigation on each aforementioned spin-up sequence have been lacking due to the temporal limitation of observation data.
- A special high-spatial/temporal-resolution and model/ observation-consistent dataset for Sinlaku was constructed by using a newly developed vortex initialization scheme (WRF-based EnKF data assimilation) and unique data collected during T-PARC.

Objectives

Part II

- **Proposing a new paradigm for SEF based on an axisymmetric view.**
  (Unbalanced response within and just above the boundary layer.)

Broadening of the tangential wind

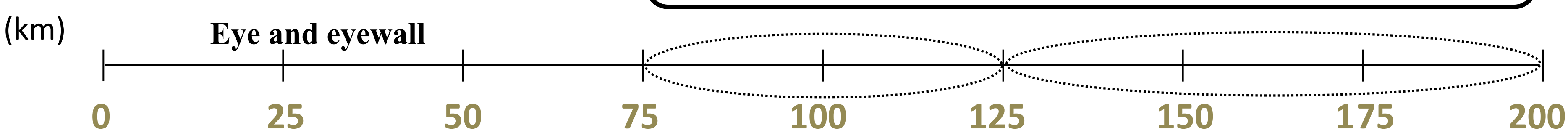

Unbalanced response within and just above the boundary layer (BL) ?

(Huang et al. 2012, JAS)

PRECURSORS PRIOR TO SEF

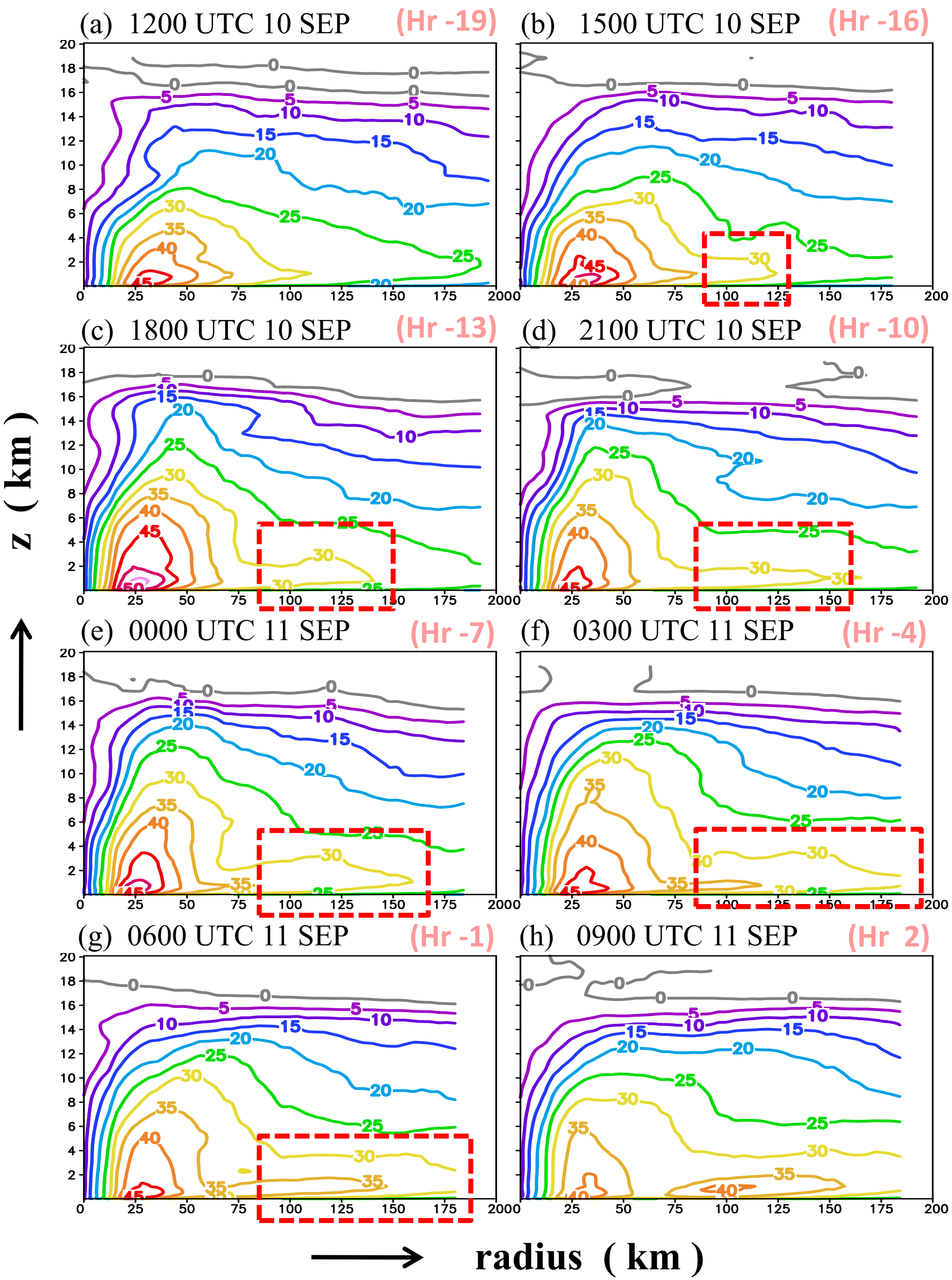

Azimuthally-mean tangential wind

r = 0 - 200 km ; z = 0 - 20 km

Broadening of the outer-core tangential wind above and within the BL prior to SEF

Fig. 1. Radius-height cross-sections of the azimuthally-averaged tangential winds (Unit: ms^{-1}), with a 5-ms^{-1} counter interval. Analyses from 1200 UTC 10 SEP to 0900 UTC 11 SEP are displayed with a 3-h interval. As defined in Part I, the secondary eyewall forms at 0700 UTC 11 SEP.

(Huang et al. 2012, JAS)

Absolute angular momentum (M) and radial flow (u)

r = 0 - 200 km ; z= 0 - 5 km

$$M = rv + \frac{1}{2} f r^2 \qquad v = \frac{M}{r} - \frac{1}{2} f r$$

1 hr prior to SEF

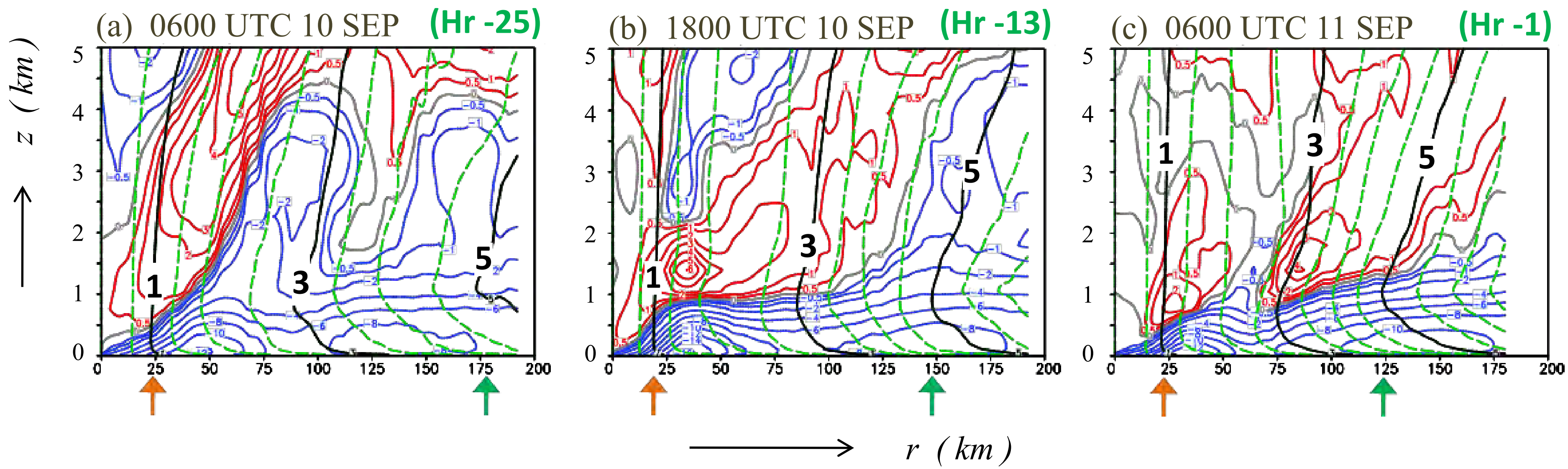

- Persistent and sufficiently large boundary layer inflow over the outer-core region.
- *M* advected inwards by persistent and sufficiently large boundary layer inflow

(Huang et al. 2012, JAS)

DYNAMICAL INTERPRETATION

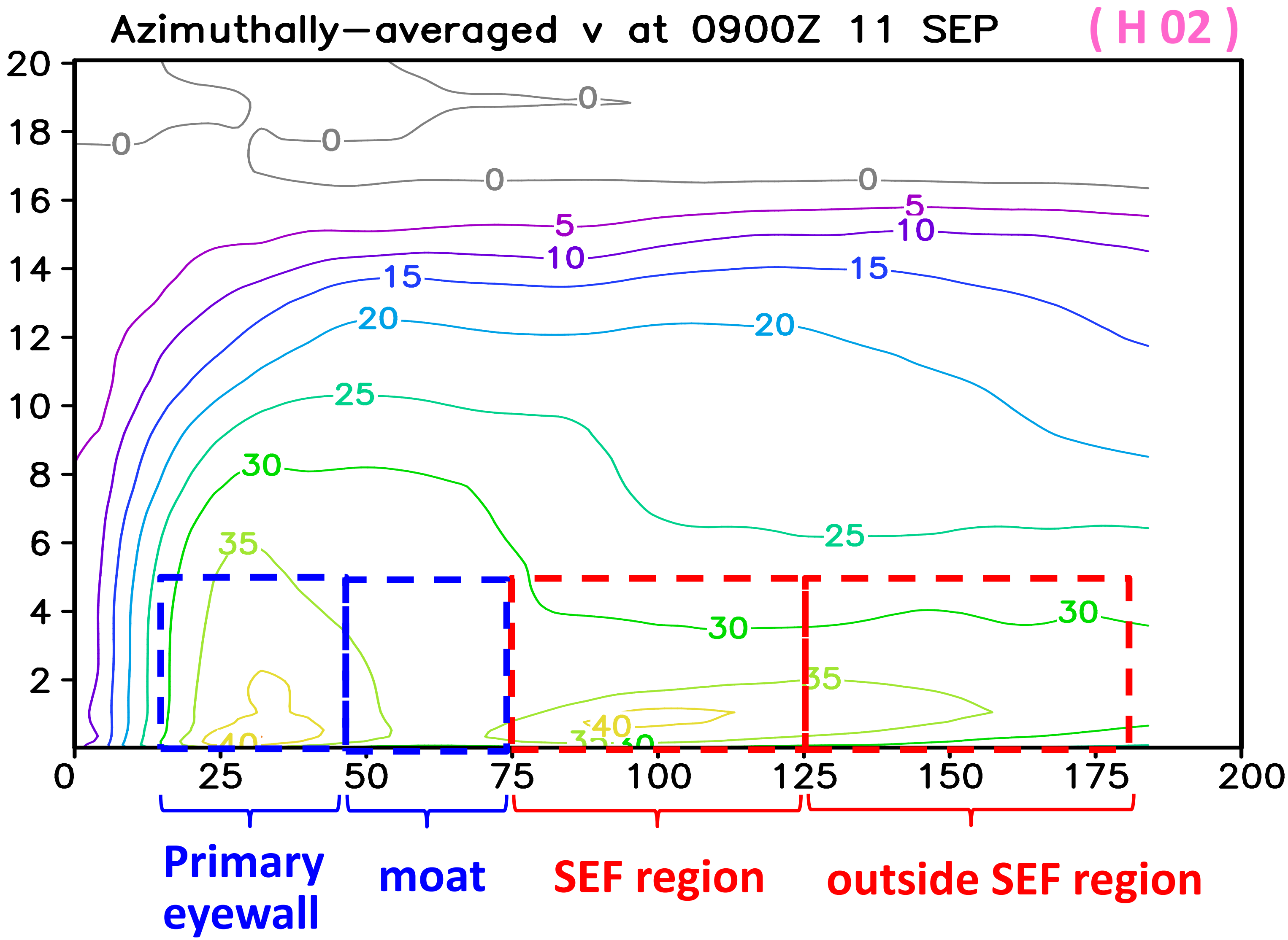

CTL

Vertical profiles of azimuthally-, area- and temporally-averaged radial flow (u) and agradient wind (V_{ag})

Increasing boundary-layer inflow $\bar{u}$

Increasing supergradient wind near the top of the boundary layer

$$\bar{V}_{ag} = \bar{V} - \bar{V}_g$$

Gradient wind balance relationship

$$\frac{\bar{V}_g^{\,2}}{r} + f\bar{V}_g = \frac{1}{\bar{\rho}}\frac{\partial \bar{p}}{\partial r}$$

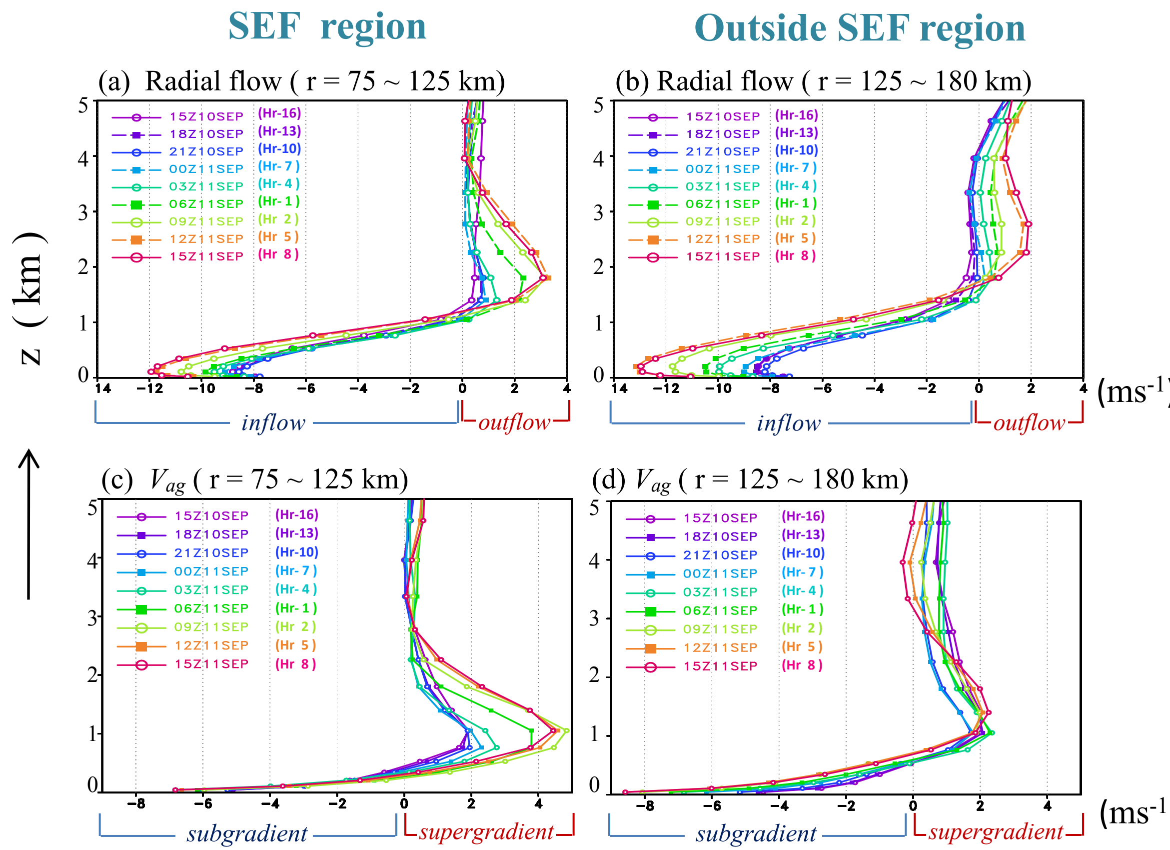

Fig.5. Azimuthally-, area- and temporally-averaged values over (t - 3 h, t + 3 h) based on 30-min output data. (a) and (b) are radial velocity (Unit: ms^{-1}); (c) and (d) are agradient wind (V_{ag} ; unit: ms^{-1}). The left panel shows the value averaged within the radial interval 75 km < r < 125 km (the SEF region), while the right panel shows the value averaged within the radial interval 125 km < r < 180 km (exterior to the SEF region). Analyses from 1500 UTC 10 SEP to 1500 UTC 11 SEP are displayed with a 3-h interval. The green line is 1 h prior to SEF, while the light-green line is 2 h after SEF.

(Huang et al. 2012, JAS)

Vertical profiles of azimuthally-, area- and temporally-averaged agradient force (AF) and radial pressure gradient force (PGF)

CTL

$(ms^{-1}h^{-1})$

$$\frac{du}{dt} = \left[\boxed{-\frac{1}{\rho}\frac{\partial P}{\partial r}} + \left(\frac{v^2}{r} + fv\right) \right] - Fr$$

PGF

AF

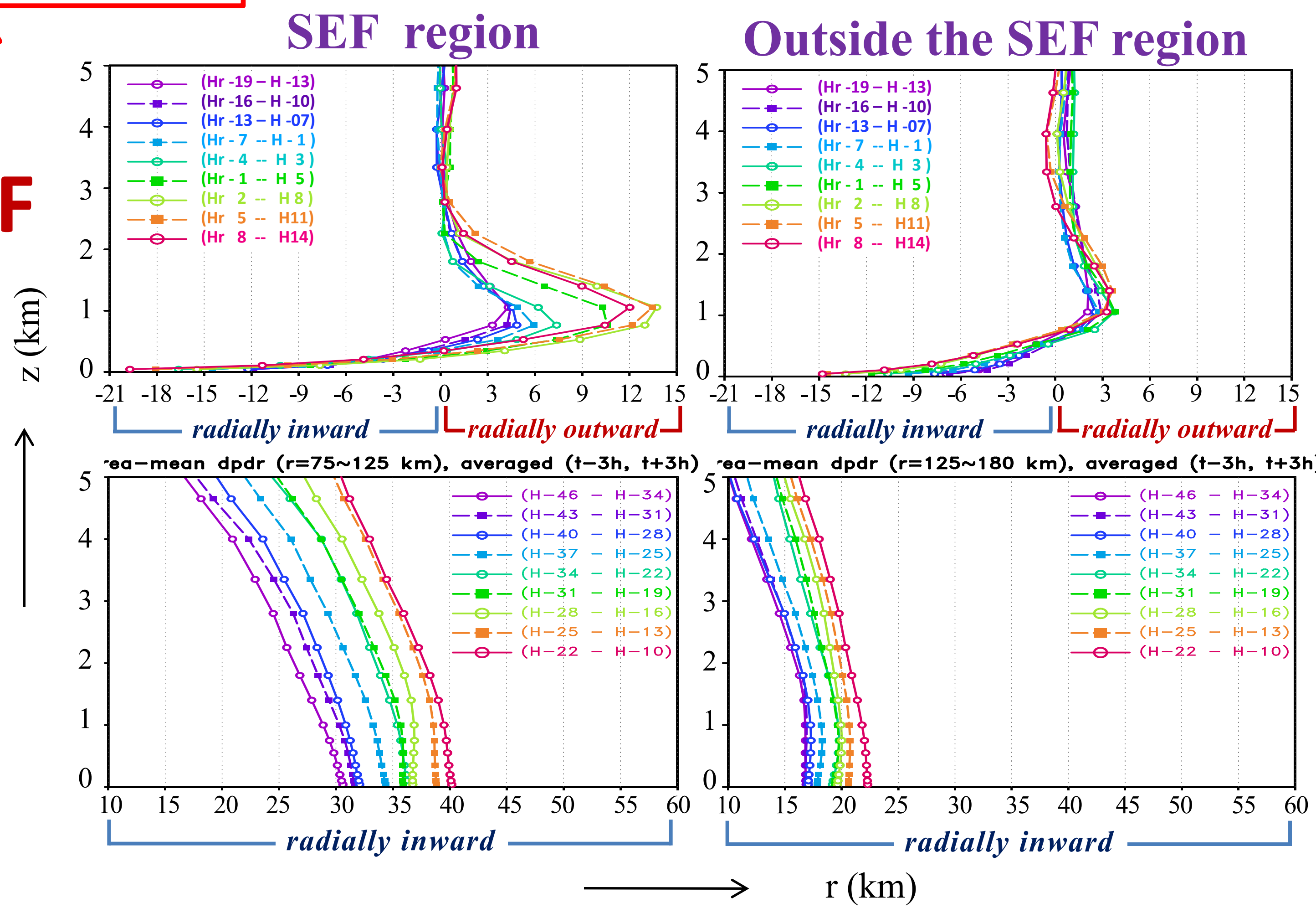

Fig. 6. Same as Fig. 5, but (a) and (b) are the agradient force (AF), while (c) and (d) are the radial pressure gradient force. Unit for these two parameters is ms-1h-1.

(Huang et al. 2011, JAS)

Vertical profiles of azimuthally-, area- and temporally-averaged **divergence** and **vertical velocity**

Divergence

Vertical velocity

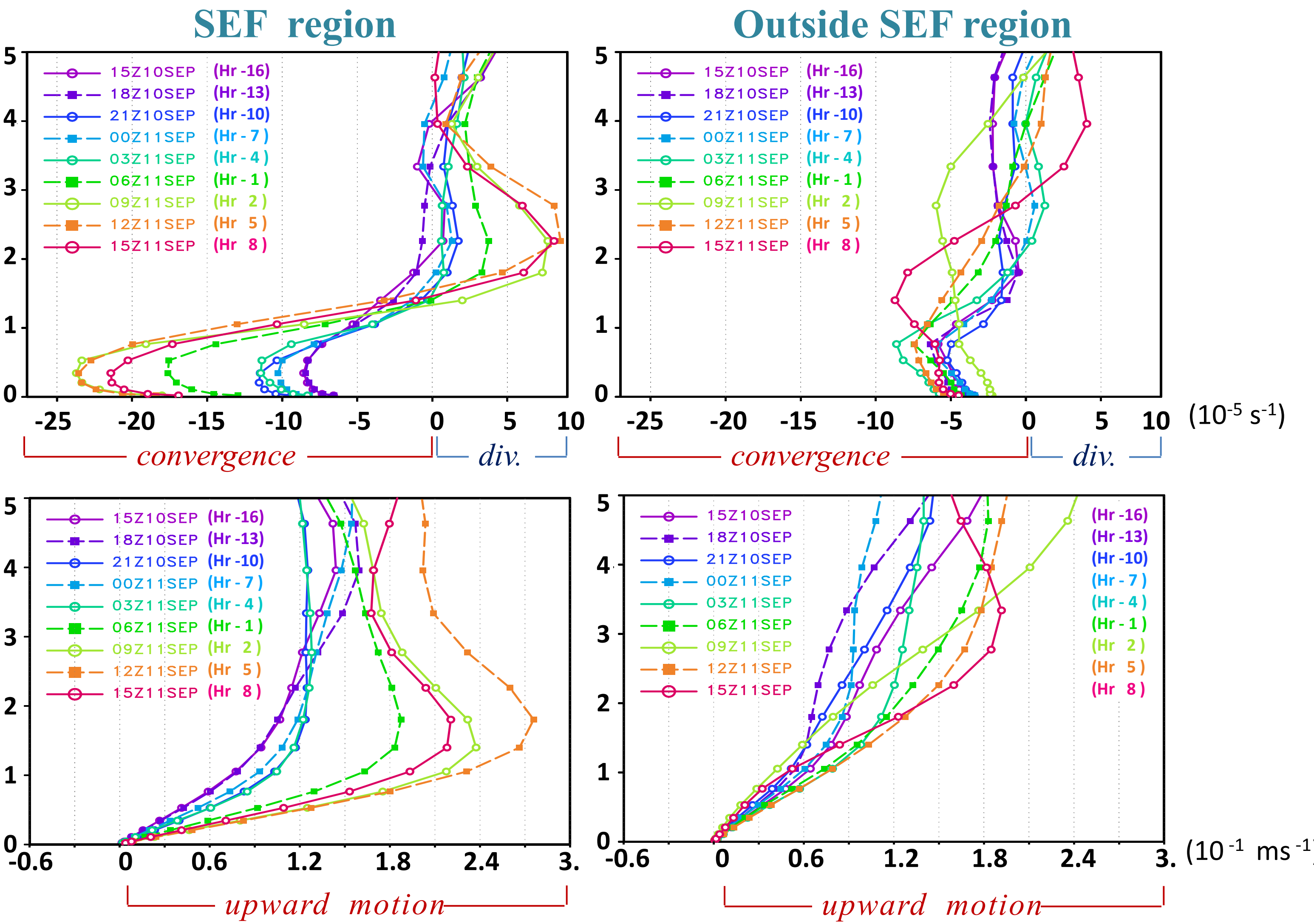

Increasing convergence within and just above the boundary layer is associated with increasing ascending motion in the lower troposphere within the SEF region.

(Huang et al. 2012, JAS)

6-hr averaged *divergence* (at 500-m) and *vertical velocity* (at 1.5-km)

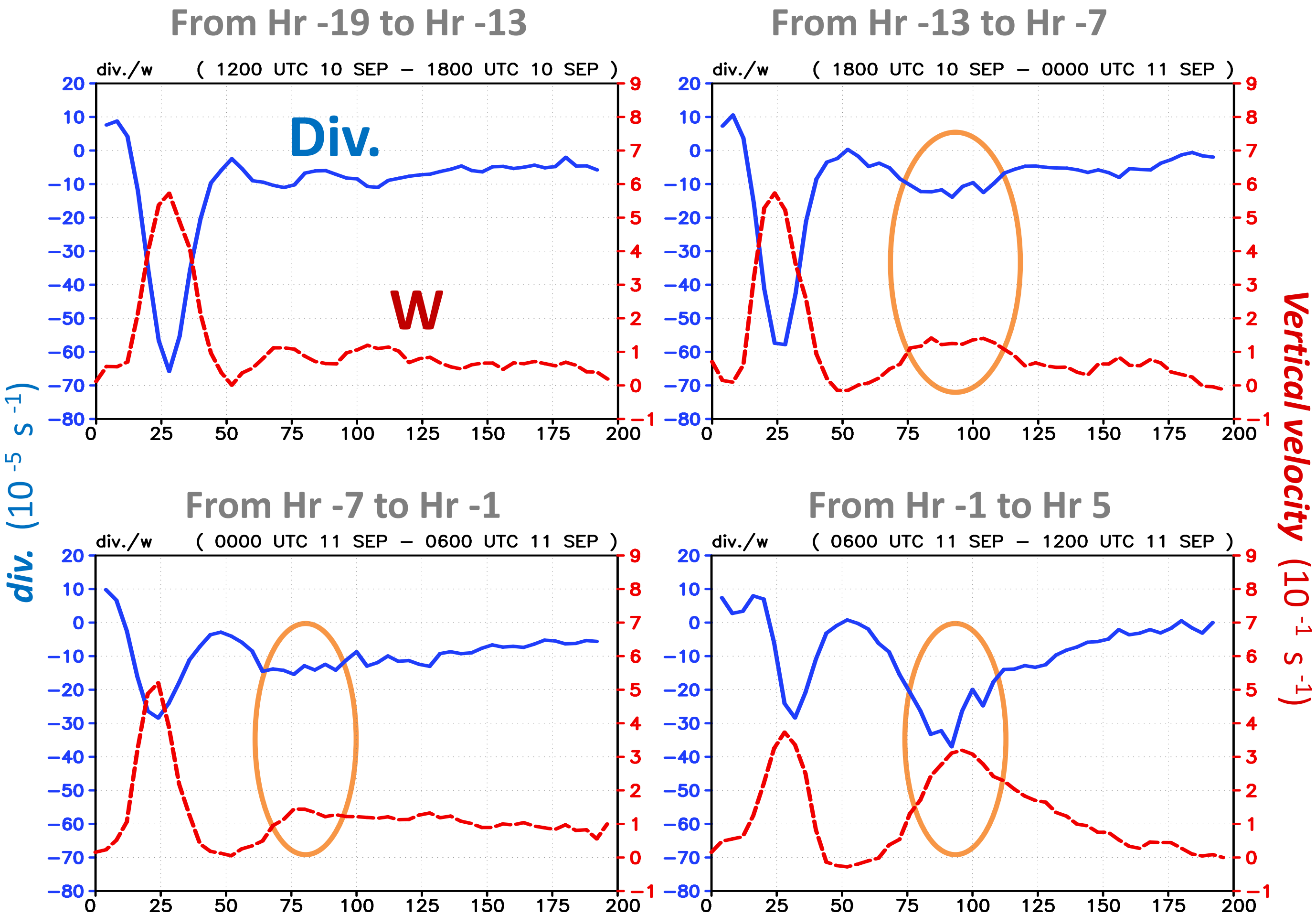

Convergence zone and upward motion are persistently stronger in SEF region over the vortex's outer core .

Regions of convergence within the boundary layer agree well with the radial distribution of the ascending motion at the lower troposphere.

Vertical profiles of azimuthally-, area- and temporally-averaged radial flow (u)

CTL

Primary Eyewall

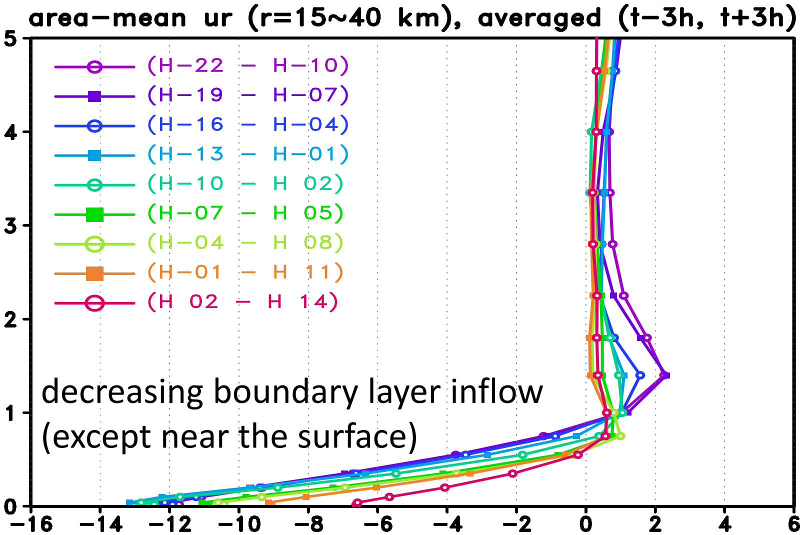

Moat Region (no or weak precipitation)

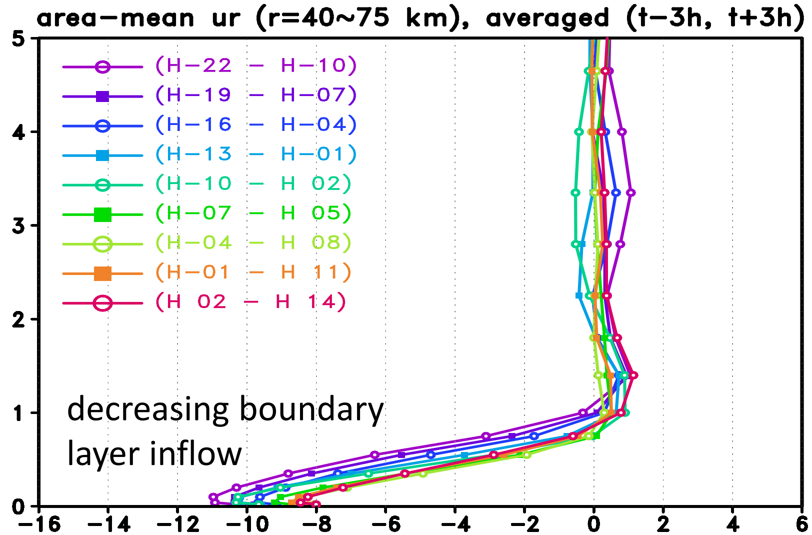

Secondary Eyewall Formation Region (SEF)

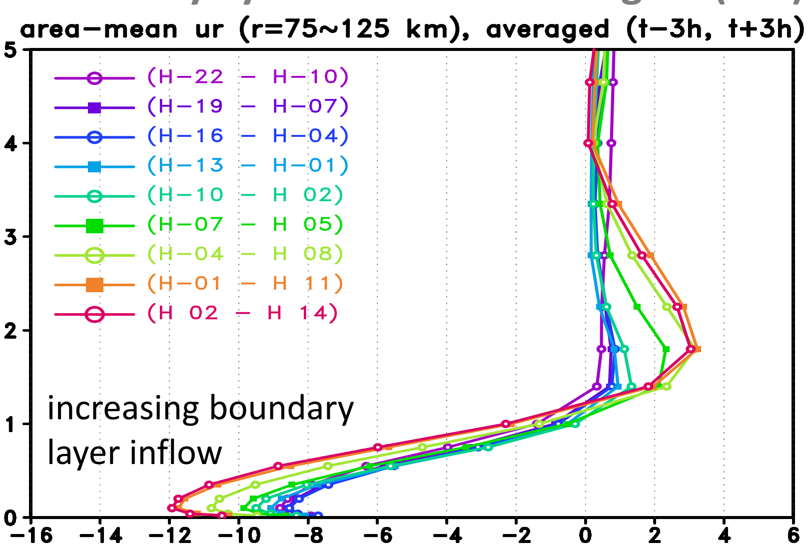

Outside SEF Region

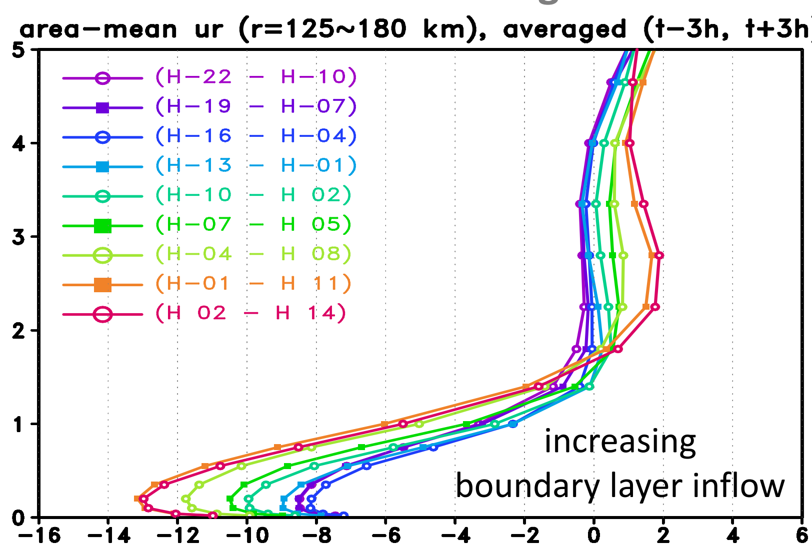

Complementary results from other independent studies

- Using data collected during RAINEX (Hurricane Rainband and Intensity Experiment), recent observational studies on Hurricane Rita (2005) have shown some supporting evidences within the secondary eyewall.
  - Didlake and Houze (2011): Apparent supergradient tangential winds found at 500-m altitude within Rita's secondary eyewall.
  - Bell et al. (2011): 1) The maximum tangential wind within the boundary layer; 2) the alternating regions of convergence (i.e., eyewalls) and divergence (i.e., the eye and moat) 150-m height agree well with the radial distribution of vertical motion.

Didlake and Houze (2011)

Supergradient winds within the primary eyewall

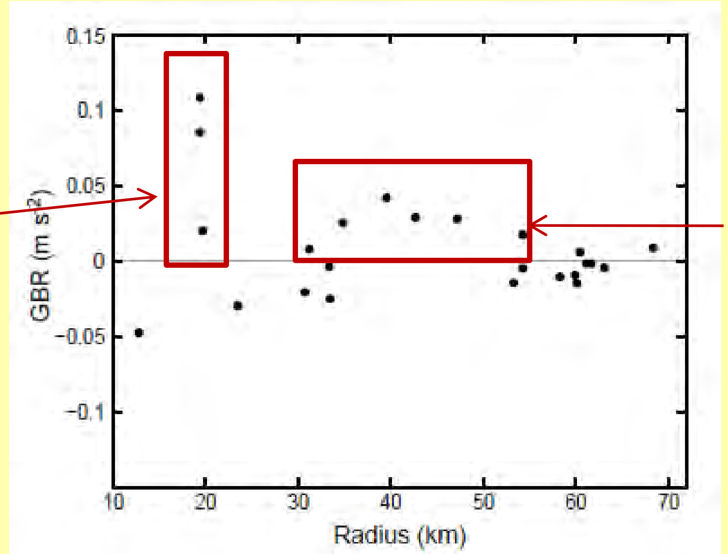

(dropsonde data)

Supergradient winds within the secondary eyewall

Bell et al. (2011)

upward motion within two eyewalls

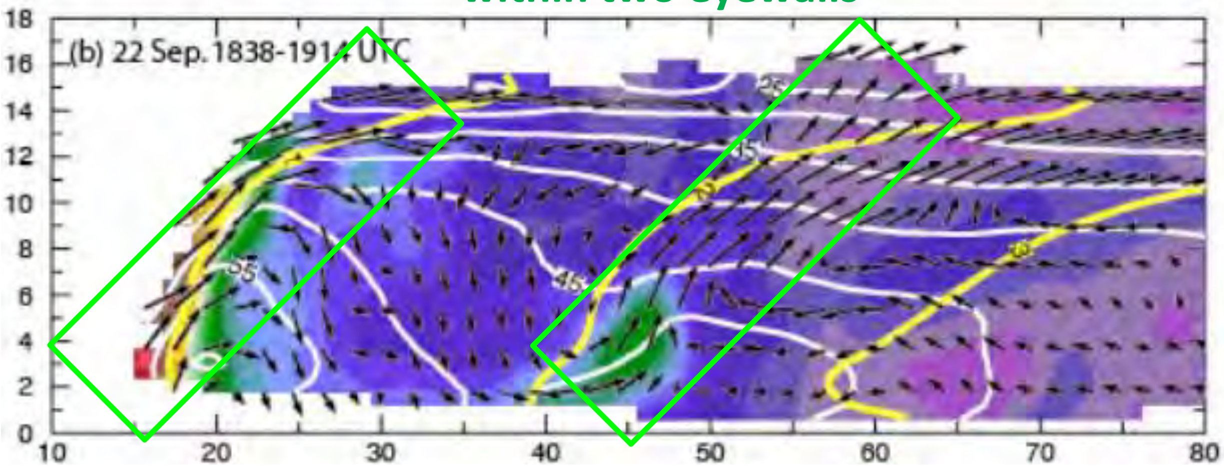

(Derived from the ELDORA Doppler Radar)

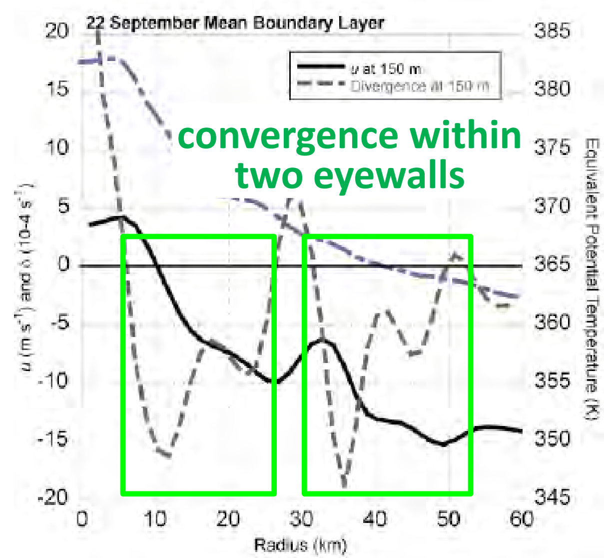

(dropsonde data)

Summary (i)

Part II (Huang et al. 2012, JAS)

- Analyses of one representative simulation from the 28 members are conducted.

- A deeper understanding of the underlying dynamics of SEF has been obtained based on some recently developed insights on the axisymmetric dynamics of tropical cyclone intensification.

- The findings point to a sequence of structural changes in the outer-core region of a mature tropical cyclone, which culminates in the formation of a secondary eyewall.

The deepening of the storm and/or convective activities in rainbands contribute to the radial gradient of the diabatic heating rate.

(Smith et al. 2009, QJRMS)

Persistent and sufficiently large inflow

M is converged inward with minimal loss to surface friction → Broadening of the tangential wind

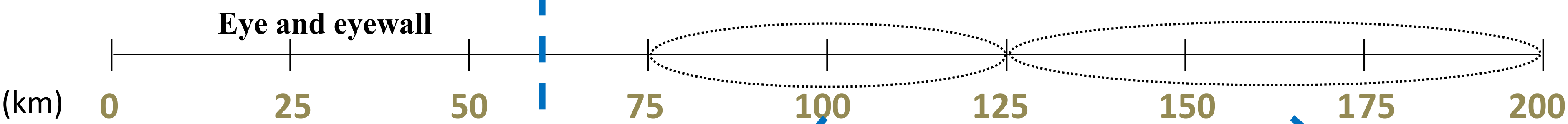

supergradient wind monotonically increase

u rapidly decelerated inward

From "sporadic and/or weak" convergence to "well-defined and concentrated" convergence zone

eruption of air out of the BL to initiate and sustain deep convection

No significant changes

$$M = rv + \frac{1}{2}fr^2$$

$$v = \frac{M}{r} - \frac{1}{2}fr$$

Unbalanced response within and just above the boundary layer (BL)

(Wu et al. 2012b, MWR; Huang et al. 2012, JAS)

⇨ **SEF** In a favorable thermodynamic and kinematic environment

Sawyer Eliassen equation

$$\frac{\partial}{\partial r^*}\left(\frac{\mathrm{Ri}N^{*2}}{r^*\rho^*}\frac{\partial\psi}{\partial r^*} - \frac{S^*\xi^*}{r^*\rho^*}\frac{\partial\psi}{\partial z^*}\right) + \frac{\partial}{\partial z^*}\left(\frac{\zeta^*\xi^*}{r^*\rho^*}\frac{\partial\psi}{\partial z^*} - \frac{S^*\xi^*}{r^*\rho^*}\frac{\partial\psi}{\partial r^*}\right) = \underbrace{-\frac{\partial}{\partial z^*}(\xi^*\mathbf{V}^*)}_{\text{momentum}} + \underbrace{\frac{\partial}{\partial r^*}\mathbf{B}^*}_{\text{heat}},$$

barotropic vortex weak I^2

Barotropic vortex strong I^2

baroclinic vortex

heat

momentum

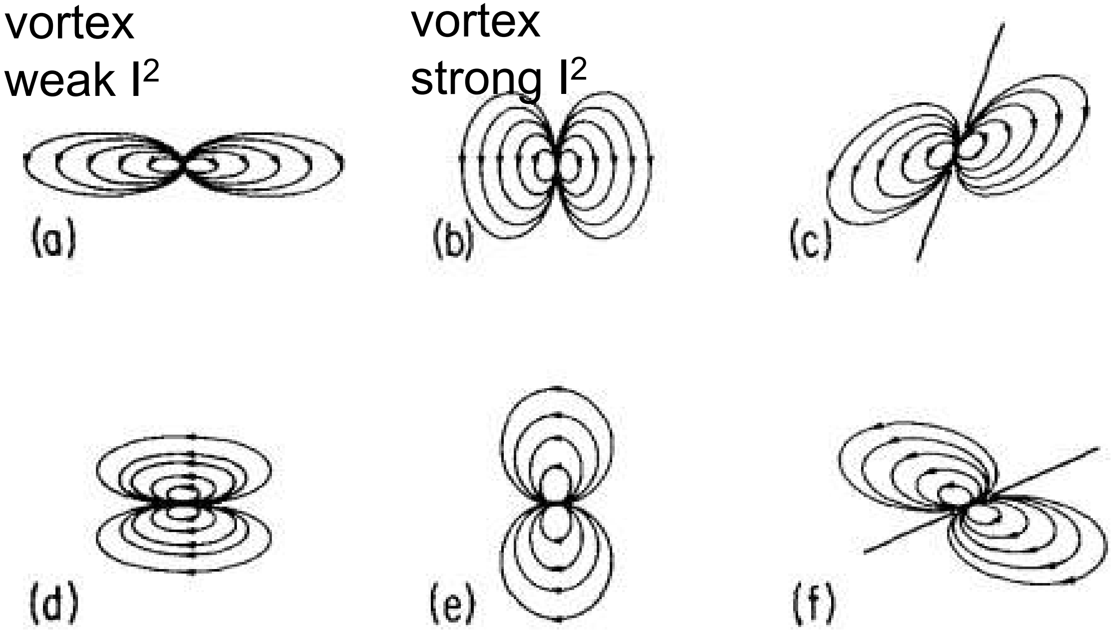

(Shapiro and Willoughby 1982

Balanced response of Sawyer Eliassen equation in typhoon

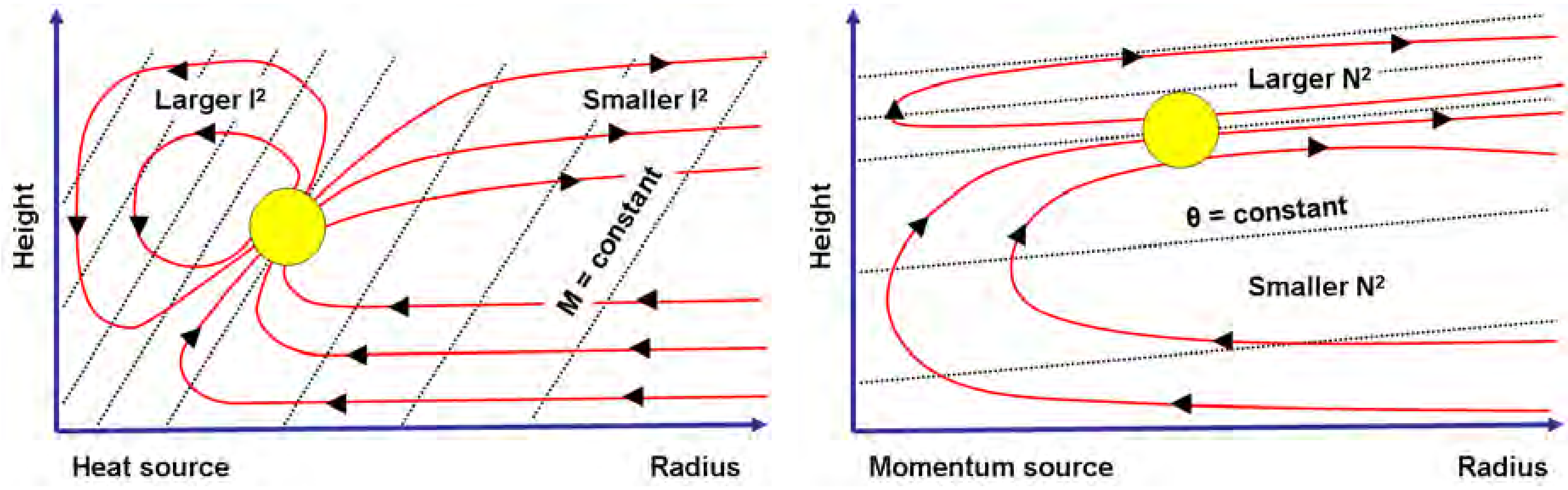

(Montgomery and Smith 2011)

Are the kinetic/thermodynamic conditions in the SEF region conducive for the development of convections?

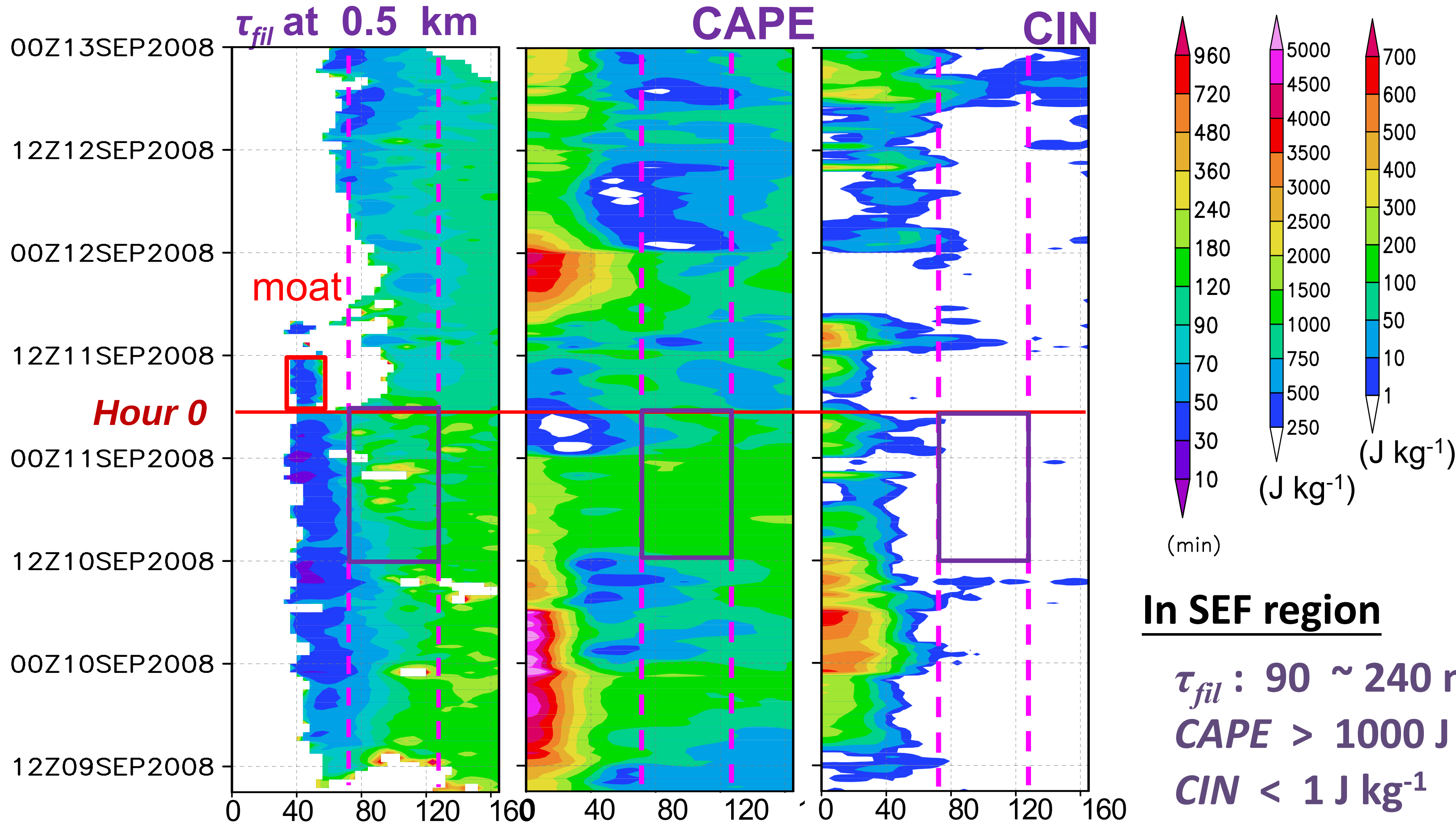

In SEF region

τ_{fil} : 90 ~ 240 min

CAPE > 1000 J kg^{-1}

CIN < 1 J kg^{-1}

In the SEF region

- ✓ Straining effect and CIN are not adverse for the development of convection.
- ✓ CAPE is in favor of the development of convection.

➔ **A convectively favorable region**

Summary (ii)

- An attractive paradigm on physical grounds because of its simplicity and consistency with the 3-D numerical simulations presented.

- Application of the two spin-up mechanisms set the scene for a progressive boundary layer control pathway to SEF.

- *The unbalanced boundary layer response to an expanding swirling wind field is an important mechanism for concentrating and sustaining deep convection in a narrow supergradient-wind zone in the outer-core region of a mature tropical cyclone.*

- The boundary layer and its coupling to the interior flow is a key process that needs to be adequately represented in numerical models to improve the understanding of SEF, as well as the accuracy of SEF forecasts, including its timing and preferred region.

Issues to be investigated

- **Is the result representative? Would the result be the artifact of data assimilation?**
  → Analyses of data-denial forecast experiments
- **How important is the mean-field dynamics?**
  → Budget calculations of the tangential wind
- Impact of model resolution (horizontal and vertical): in data-denial experiments
- Impact of physical process (convection vs. PBL process)
- Conducting Sawyer-Eliassen diagnostics to investigate the balanced and unbalanced responses of the secondary circulation to the radial gradient of diabatic heating.
- Insights into the design of more idealized experiments

Objectives

Part I

- Constructing a dataset for Typhoon Sinlaku by using T-PARC data and a new vortex initialization method via the WRF model.
- **Showing the evolution of the concentric eyewall cycle in terms of different parameters.**.

Part II

- **Investigating potential precursors to SEF and providing a corresponding dynamical interpretation.**
- **Proposing a new pathway to SEF based on an axisymmetric view.** ***(Unbalanced response within and just above the boundary layer.)***

Part III

- **Validating the presenting pathway in the data-denial experiments.**

Data-denial forecast experiments

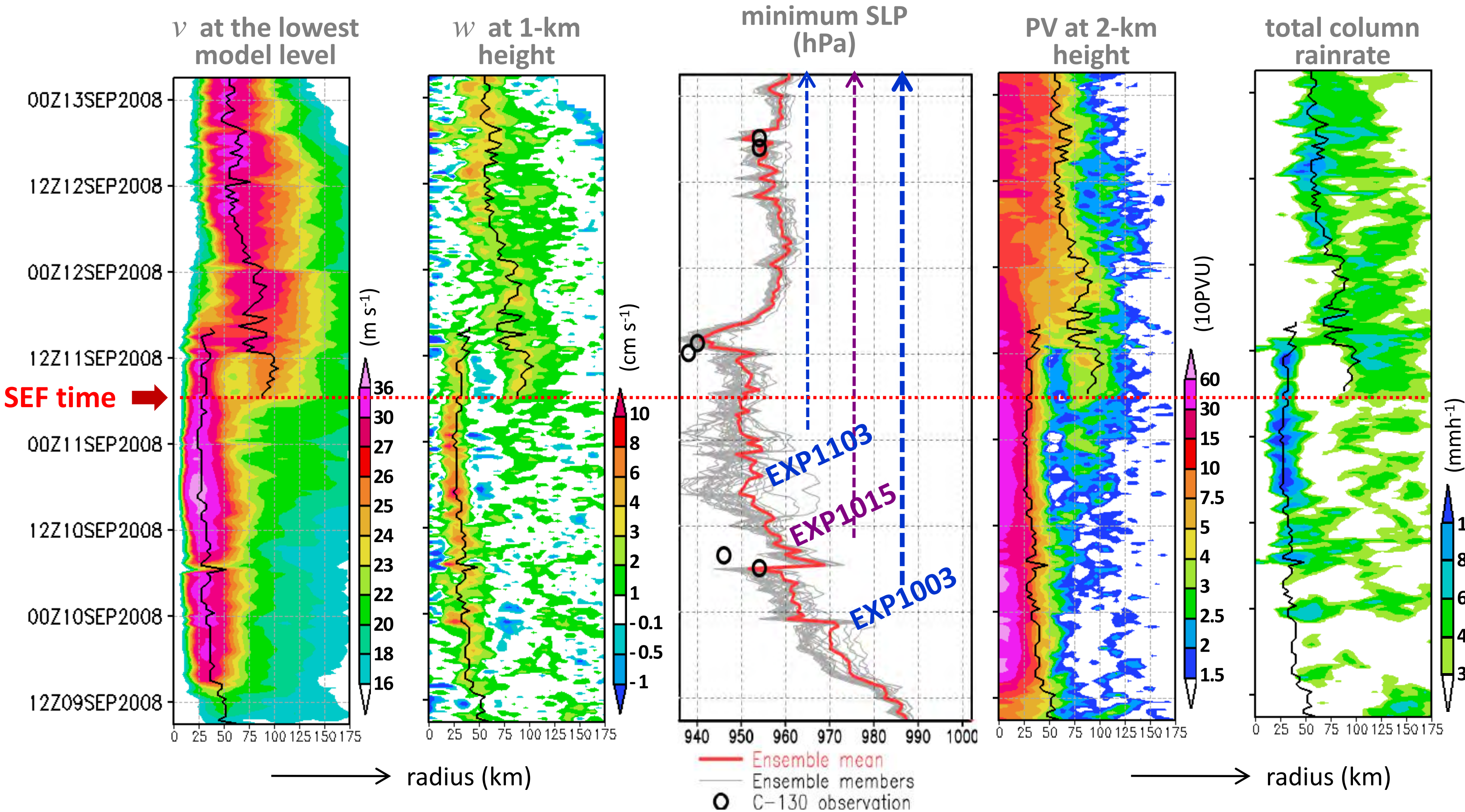

SEF time: a persistent secondary maximum in *V* at the lowest model level

Hr -1 : 1 h prior to SEF ; Hr 0 : SEF time ; Hr 1: 1 h after SEF

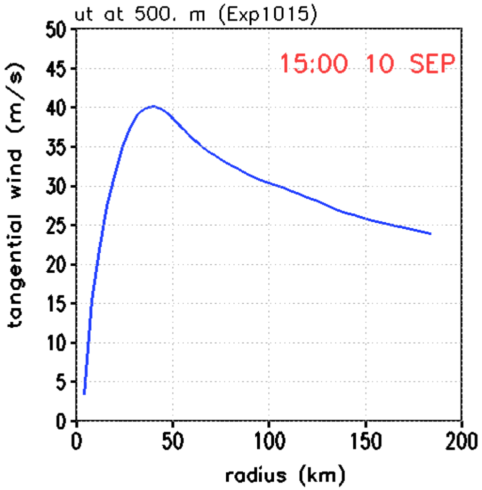

EXP1015

data ingest suppressed after 1500 UTC 10 SEP

azimithal-mean v profile
plane view of v and PV
time-radius plots

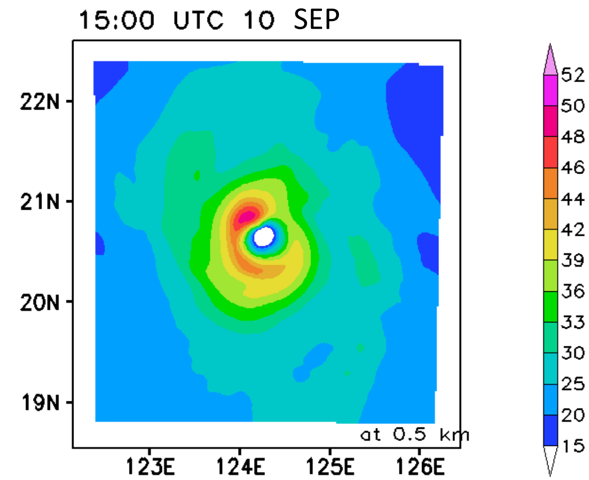

sporadic convective cells

concentric eyewalls

New eyewall

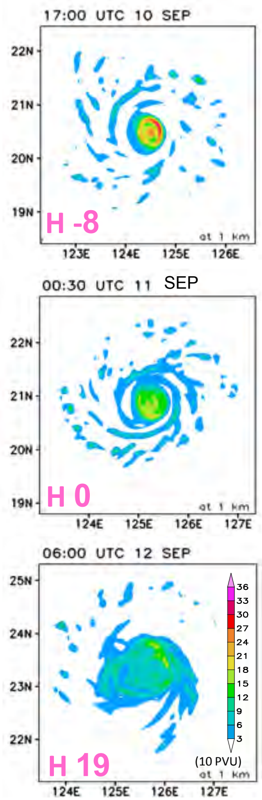

CE structure (less distinct); SEF time: 0100 UTC 11 SEP

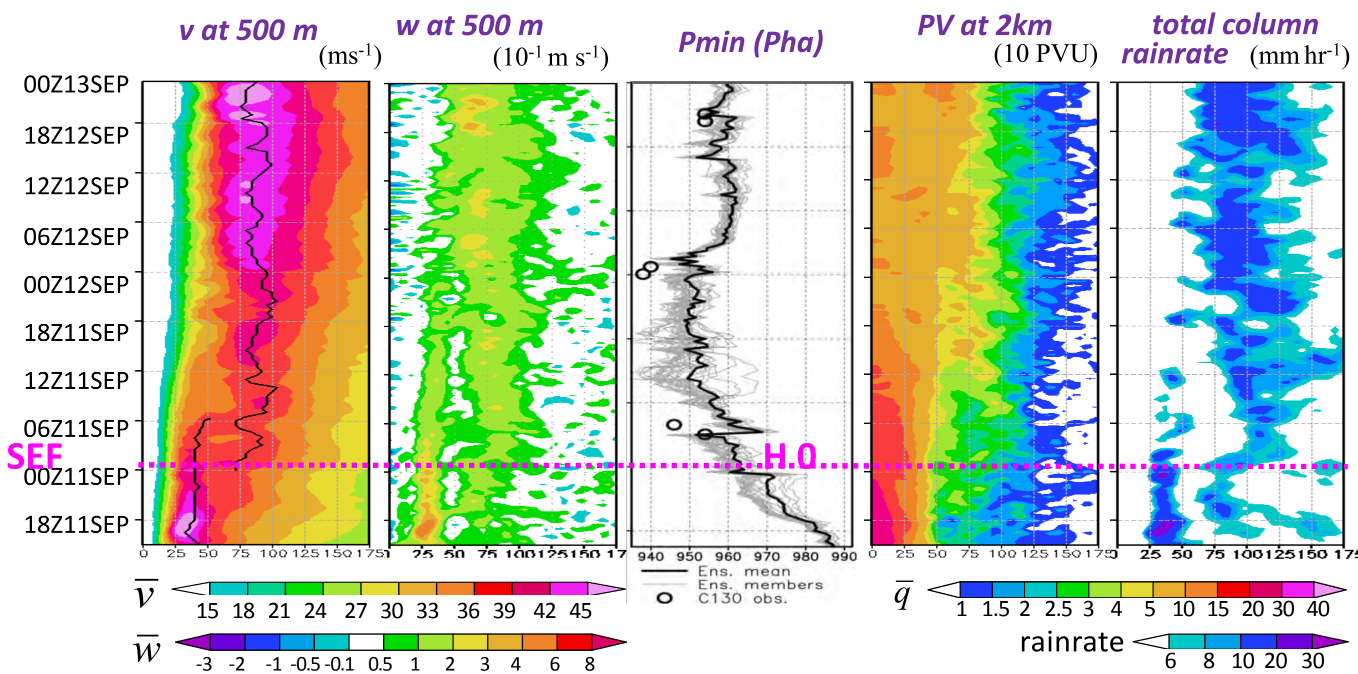

(Wu et al. 2012a, MWR)

References

Abarca, S. F., and K. L. Corbosiero, 2011: Secondary eyewall formation in WRF simulations of hurricanes Rita and Katrina (2005). *Geophys. Res. Lett.*, **38**, L07802, doi:10.1029/2011GL047015. Chen, Y., and M. K. Yau (2001), Spiral bands in a simulated hurricane. Part I: Vortex Rossby wave verification, *J. Atmos. Sci.*, **58**, 2128-2145.

____, G. Brunet, and M. K. Yau (2003), Spiral bands in a simulated hurricane. Part II: Wave activity diagnostics, *J. Atmos. Sci.*, **60**, 1239-1256. Hawkins, H. F., 1983: Hurricane Allen and island obstacles, *J. Atmos. Sci.,* **40**, 1360–1361.

Corbosiero, K. L., J. Molinari, A. R. Aiyyer, and M. L. Black, 2006: The structure and evolution of Hurricane Elena (1985). Part II: Convective asymmetries and evidence for vortex Rossby waves. *Mon. Wea. Rev*., **134**, 3073–3091.

____, S. Arbaca, and M. T. Montgomery, 2012: Vortex Rossby waves and secondary eyewall formation in a high-resolution simulation of Hurricane Katrina (2005). *30th Conference on Hurricanes and Tropical Meteorology, American Meteorological Society*, Jacksonville, FL , Amer. Meteor. Soc., 1A.6.

Hill, K. A., and G. M. Lackmann, 2009: Influence of environmental humidity on tropical cyclone size. *Mon. Wea. Rev*., **137**, 3294-3315.

Huang, Y.-H., M. T. Montgomery, C.-C. Wu, 2012: Concentric eyewall formation in Typhoon Sinlaku (2008). Part II: Axisymmetric dynamical processes. *J. Atmos. Sci.*, **69**, 662-674.

Kuo, H.-C., L.-Y. Lin, C.-P. Chang, and R. T. Williams, 2004: The formation of concentric vorticity structures in typhoons. *J. Atmos. Sci.*, **61**, 2722–2734.

____, C.-P. Chang, Y.-T. Yang, and H.-J. Jiang, 2009: Western North Pacific Typhoons with Concentric Eyewalls. *Mon. Weather Rev.,***137**, 3758-3770.

Menelaou, Konstantinos, P. M. K. Yau, and Y. Martinez,2012: On the dynamics of secondary eyewall formation in Hurricane Wilma (2005). *30th Conference on Hurricanes and Tropical Meteorology, American Meteorological Society*, Jacksonville, FL , Amer. Meteor. Soc., 1A.1.

McWilliams, J. C., 1990: The vortices of two-dimensional turbulence. *J. Fluid. Mech.*, **219**, 361-385.

Martinez, Y., G. Brunet, M. K. Yau, and X. Xang, 2011: On the dynamics of concentric eyewall genesis: Space-time empirical normal modes diagnosis. *J. Atmos. Sci*., **68**, 457-476.

Montgomery, M. T., and J. Enagonio, 1998: Tropical cyclogenesis via convectively forced vortex Rossby waves in a three-dimensional quasigeostrophic model. *J. Atmos. Sci.,* **55**, 3176–3207.

Moon, Y. D. S. Nolan, and M. Iskandarani, 2010: On the use of two-dimensional incompressible flow to study secondary eyewall formation in tropical cyclones. *J. Atmos. Sci.*, **67**, 3765–3773.

Nong, S., and K. A. Emanuel, 2003: A numerical study of the genesis of concentric eyewalls in hurricane. *Quart. J. Roy. Meteor. Soc.*, **129**, 3323–3338.

Ortt, D., and S. S. Chen, 2008: Effect of environmental moisture on rainbands in Hurricane Rita and Katrina (2005). *28th Conference on Hurricanes and Tropical Meteorology, American Meteorological Society*, Miami, FL , Amer. Meteor. Soc., preprint 5C.5.

Qiu, X., Z.-M Tan, and Xiao Q., 2010: The Roles of Vortex Rossby Waves in Hurricane Secondary Eyewall Formation. *Mon. Weather. Rev.,* **138**, 2092-2109.

Rozoff, C. M., W. H. Schubert, B. D. McNoldy, and J. P. Kossin, 2006: Rapid filamentation zones in intense tropical cyclones. *J. Atmos. Sci*., **63**, 325–340.

____., D. S. Nolan, J. P. Kossin, F. Zhang, and J. Fang: The roles of an expanding wind field and inertial stability in tropical cyclone secondary eyewall formation. *J. Atmos. Sci*. (in press).

Terwey, W. D., and M. T. Montgomery, 2008: Secondary eyewall formation in two idealized, full-physics modeled hurricanes. *J. Geophys. Res.*, **113**, D12112. Willoughby, H. E., 1979: Forced secondary circulations in hurricanes, *J. Geophys. Res.*, **84**, 3173– 3183.

Willoughby, H. E., 1979: Excitation of Spiral Bands in Hurricanes by Interaction Between the Symmetric Mean Vortex and a Shearing Environmental Steering Current. *J. Atmos. Sci.,* **36**, 1226-1235

Willoughby, H. E., J. A. Clos, and M. G. Shoreibah, 1982: Concentric eyewalls, secondary wind maxima, and the evolution of the hurricane vortex, *J. Atmos. Sci.*, **39**, 395– 411.

____, H.-L. Jin, S. J. Lord, and J. M. Piotrowicz, 1984: Hurricane structure and evolution as simulated by an axisymmetric, nonhydrostatic numerical model, *J. Atmos. Sci.*, **41**, 1169–1186.

Wang, X., Y. Ma, and N. E. Davidson, 2012: Secondary eyewall formation and eyewall replacement cycles in a simulated storm: Effect of unbalanced forces in the atmospheric boundary layer. (submitted to JAS)

Wang, Y., 2002a: Vortex Rossby waves in a numerically simulated tropical cyclone. Part I: Overall structure, potential vorticity, and kinetic energy budgets. *J. Atmos. Sci.*, **59**, 1213–1238.

____, 2002b: Vortex Rossby waves in a numerically simulated tropical cyclone. Part II: The role in tropical cyclone structure and intensity changes. *J. Atmos. Sci.*, **59**, 1239–1262.

____, 2009: How do outer spiral rainbands affect tropical cyclone structure and intensity? *J. Atmos. Sci.*, **66**, 1250-1273.

Wu, C.-C., Y.-H Huang, and G.-Y. Lien, 2012a: Concentric eyewall formation in Typhoon Sinlaku (2008). Part I: Assimilation of T-PARC data based on the ensemble Kalman filter (EnKF). *Mon. Wea. Rev.*, **140**, 506-527.

____, Y.-H Huang and M. T. Montgomery, 2012b: Concentric eyewall formation in Typhoon Sinlaku (2008). Part II: Further examination of axisymmetric and asymmetric processes. *30th Conference on Hurricanes and Tropical Meteorology, American Meteorological Society*, Jacksonville, FL , Amer. Meteor. Soc., 1A.4.

Zhou, Xiaqiong, Bin Wang, 2011: Mechanism of concentric eyewall replacement cycles and associated Intensity Change. *J. Atmos. Sci.,* **68,** 972–988.

Issues to be investigated

- **Is the result representative? Would the result be the artifact of data assimilation?**
  → Analyses of data-denial forecast experiments

- **How important is the mean-field dynamics?**
  → Budget calculations of the tangential wind

- Impact of model resolution (horizontal and vertical): in data-denial experiments

- Impact of physical process (convection vs. PBL process)

- Conducting Sawyer-Eliassen diagnostics to investigate the balanced and unbalanced responses of the secondary circulation to the radial gradient of diabatic heating.

- Insights into the design of more idealized experiments

$\bar{v}$ budget analysis : $\frac{\partial \bar{v}}{\partial t} = -\bar{u}\overline{\zeta_{abs}} - \bar{w}\frac{\partial \bar{v}}{\partial z} - \overline{u'\zeta'_{abs}} - \overline{w'\frac{\partial v'}{\partial z}} + F_{fric}$

(0) (a) (b) (c) (d) (e)

based on 2-min output data
(Unit: $ms^{-1} h^{-1}$)

H -19 – H -10 **H -10 – H -01**

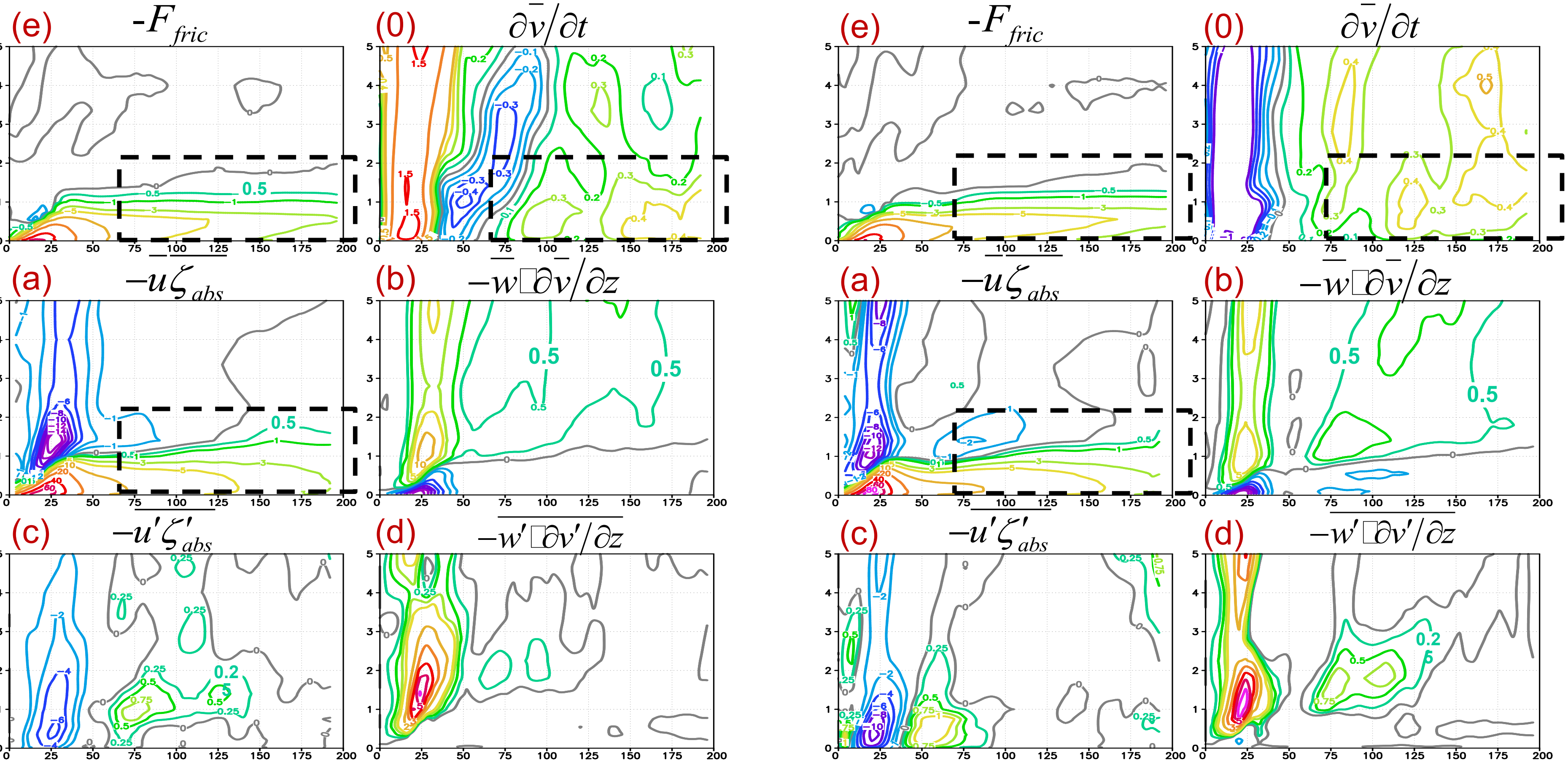

In the SEF region (75 – 125 km)

- **Within the inflow layer, the mean component of the radial advection outweighs the frictional loss.**
- **Above the inflow layer, the mean and asymmetric components enhance the tangential winds.**

The mean radial advection in absolute vorticity plays the dominant role in enhancing the tangential wind near the top of the boundary layer.

Ongoing works

- Sawyer-Eliassen diagnostics to evaluate the balanced and unbalanced responses of the secondary circulation to the radial distribution of the diabatic heating.

  ✓ Diabatic heating in the primary eyewall

  ✓ Diabatic heating projection from the rainbands or small-scale convective features in the vortex's outer-core region.

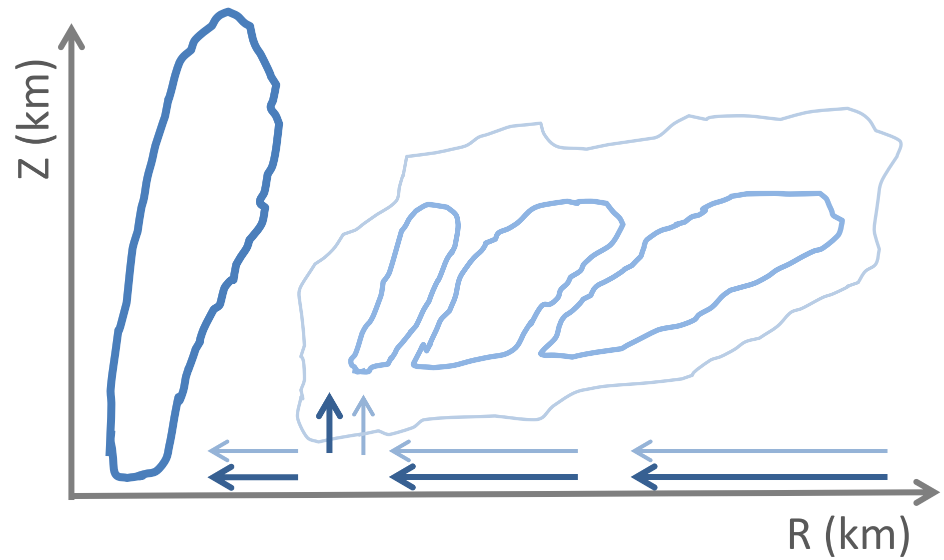

- Validation by more observation data and simulations in TCs, whether or not they have undergone SEF.
- Impact of model resolution (horizontal and vertical): in data-denial experiments
- Impact of physical process (convection vs. PBL process)
- Insights into the design of more idealized experiments

THANKS FOR LISTENING